HELSINKI UNIVERSITY OF TECHNOLOGY
Department of Electrical and Communications Engineering

Eeva Lääniläinen

Soft Lithography for Surface Micropatterning

This thesis is submitted in partial fulfilment of the requirements for the degree of Master of Science in Technology.

Espoo, 29 June 2006

Supervisor:

Professor Pekka Kuivalainen

Instructors:

Docent Sami Franssila

Ph.D. Kestutis Grigoras

Acknowledgements

First of all, I want to thank professor Pekka Kuivalainen for supervising this thesis. My gratitude also goes to my instructor, docent Sami Franssila, for giving me the opportunity to do my master's thesis on this interesting topic as well as for the ideas and supportive discussions. I also want to thank my second instructor, Dr. Kestutis Grigoras, for encouragement, valuable ideas and comments throughout the work.

I would also like to thank the personnel of Microelectronics Centre for discussions and a pleasant working environment and everyone who helped me with my work.

Finally, I would like to thank my parents and friends for love, support and encouragement.

Espoo, 29 June 2006

Eeva Lääniläinen

HELSINKI UNIVERSITY OF TECHNOLOGY Abstract of the Master's Thesis

Author: Eeva Kaisa Lääniläinen
Title of thesis: Soft Lithography for Surface Micropatterning
Date: 29.6.2006 **Pages:** 83+2

Department: Department of Electrical and Communications Engineering
Professorship: S-69 Electron Physics:

Supervisor: Professor Pekka Kuivalainen
Instructors: Docent Sami Franssila, Ph.D. Kestutis Grigoras

In the first part of this work, a literature review of soft lithographic techniques is presented. Soft lithography includes a number of techniques for the fabrication of two- and three dimensional micro- and nanostructures based on molding, embossing and printing.

In the experimental part of this work, two soft lithographic methods of surface micropatterning are used in order to produce an array of gold dots onto a substrate. The methods used are microcontact printing and transfer printing.

Different master designs and their fabrication is presented, followed by stamp fabrication. The masters are fabricated using conventional microfabrication techniques and photolithography. Master designs tested are inverted pyramid shape fabricated by anisotropic etching of silicon, a high aspect ratio master and a low aspect ratio photoresist master. The elastomeric stamps are negative replicas of the masters and they are fabricated of poly(dimethylsiloxane) (PDMS). The stamps have a regular array of protruding features, in order to make a contact to the substrate during printing.

Stamp designs chosen for microcontact printing are the pyramid stamp and the low aspect ratio stamp. In microcontact printing experiments eicosanethiol solution is used as the ink with which the stamp is wetted and the pattern of the stamp printed onto a gold-coated substrate. Both wet and contact inking methods are tested. Eicosanethiol forms a self assembling monolayer (SAM) onto the gold surface. The printed pattern is used as an etch mask in the subsequent wet of etching gold, which is performed in a solution of thiourea and ferric(III)nitrate. After the etching, an array of gold dots remains on the substrate.

Stamp design chosen for transfer printing is the low aspect ratio stamp. In the version of transfer printing used in this work, eicosanethiol forms a layer on the silicon dioxide film, without the formation of a SAM. A gold-coated PDMS stamp is used to transfer a gold pattern onto the pre-treated silicon substrate.

The results of microcontact printing show that the features are smaller at the edges of the printed area, possibly due to uneven pressure during printing or unevenness of the stamp itself. The mask used in the fabrication of the low aspect ratio stamps was not of high enough quality to produce homogenous stamps, thus leading to a periodical size variation in the prints made with the low aspect ratio stamps. Therefore, pyramid stamp is better suited for microcontact printing of gold dots. Diffusion of the thiols causes pattern distortion in microcontact printing; contact inking diminishes diffusion and produces smaller patterns than wet inking.

In transfer printing the pattern is overall regular and smooth and the periodical size variation is not visible. The low aspect ratio stamp is well suited for transfer printing.

Both methods are suited for the gold dot array fabrication. The diameter of the dots created with these methods is in the range of $1 - 2$ μm.

Keywords: soft lithography, microfabrication, PDMS, surface patterning, self assembled monolayers, microcontact printing, transfer printing

Tekijä: Eeva Kaisa Lääniläinen
Työn nimi: Pehmeä litografia pinnan mikrokuvioinnissa
Päivämäärä: 29.6.2006 **Sivumäärä:** 83+2
Osasto: Sähkö- ja tietoliikennetekniikan osasto
Professuuri: S-69 Elektronifysiikka
Työn valvoja: Professori Pekka Kuivalainen
Työn ohjaajat: Dosentti Sami Franssila, TkT Kestutis Grigoras

Tämän työn ensimmäisessä osassa on tehty kirjallisuusselvitys pehmeän litografian menetelmistä. Pehmeää litografiaa voidaan tehdä useilla eri tekniikoilla, joilla voidaan valmistaa kaksi- tai kolmiulotteisia mikro- ja nanorakenteita. Menetelmät perustuvat muovaukseen, kohokuviointiin ja painamiseen.

Työn kokeellisessa osassa on valmistettu kahdella eri pehmeän litografian menetelmällä substraatin pinnalle kultapistematriisi. Menetelmät ovat microcontact printing ja transfer printing.

Erilaisten masterien rakenteet, sekä masterien ja stämppien valmistus on esitelty. Masterit on valmistettu perinteisillä mikrovalmistustekniikoilla ja valolitografialla. Työssä käytetyt master-rakenteet ovat ylösalainen pyramidirakenne, korkean aspektisuhteen rakenne, sekä matalan aspektisuhteen valoresistirakenne. Elastomeeristen stämppien materiaali on poly(dimetyylisiloksaani) (PDMS). Stämpeissä on säännöllinen matriisi kohollaan olevia rakenteita, joiden on tarkoitus muodostaa kontakti substraatin kanssa.

Microcontact printing -kokeisiin on valittu pyramidi- ja matalan aspektisuhteen stämpit. Eikosaanitioliliuosta on käytetty musteena jolla stämppi on kostutettu ja stämpin kuviointi on painettu kultapäällystettyyn substraattiin. Musteen levitykseen on käytetty märkä- ja kontaktimenetelmää. Eikosaanitioli muodostaa itsejärjestyvän molekyylikerroksen kullan pinnalle. Painettu kuviointi toimii etsausmaskina seuraavassa kullan märkäetsauksessa. Etsaus on suoritettu tiourea ja rauta(III)nitraatti -liuoksessa. Etsaamisen jälkeen substraatin pinnalla on kultapistematriisi.

Transfer printing -kokeisiin on valittu matalan aspektisuhteen stämppi. Tässä työssä käytetyssä versiossa eikosaanitioli muodostaa kerroksen piidioksidikerroksen päälle muodostamatta itsejärjestyvää molekyylikerrosta. Kullattua stämppiä käytetään siirtämään kultakuvio esikäsitellyn substraatin pinnalle.

Microcontact printing -kokeiden tulokset osoittavat kuvioiden olevan pienempiä kuvioidun alueen reunoilla, johtuen mahdollisesti epätasaisesta paineesta painamisen aikana tai stämpin epätasaisuudesta. Matalan aspektisuhteen stämppien valmistuksessa käytetty maski ei ollut riittävän hyvälaatuinen tuottaakseen homogeenisiä stämppejä, vaan aiheutti jaksollisen vaihtelun kuvioiden kokoon. Sen vuoksi pyramidistämppi sopii paremmin pienten pisteiden kuviointiin microcontact printing -menetelmällä. Tiolien diffuusio aiheuttaa kuvion vääristymistä microcontact printing -menetelmässä. Kontaktimenetelmällä voidaan tuottaa pienempiä kuvioita kuin märkämenetelmä.

Transfer printing -menetelmällä valmistettu kuviointi on kauttaaltaan säännöllinen ja siisti, eikä jaksollista kuvioiden koon vaihtelua ole havaittavissa. Matalan aspektisuhteen stämppi soveltuu transfer printing -menetelmään.

Kumpikin menetelmä soveltuu kultapistematriisin valmistamiseen. Näillä menetelmillä valmistettujen pisteiden halkaisija on $1 - 2\ \mu m$

Avainsanat: pehmeä litografia, mikrovalmistus, PDMS, pinnan kuviointi, itsejärjestyvä molekyylikerros, microcontact printing, transfer printing

List of Symbols and Abbreviations

BHF	buffered hydrofluoric acid
CCP	capasitively coupled plasma
CNT	carbon nanotube
CVD	chemical vapour deposition
DI-water	de-ionized water
DLC	diamond-like carbon
DLC-PDMS-h	diamond-like carbon - poly(dimethylsiloxane) - hybrid
DLC-PTFE-h	diamond like carbon - polytetrafluoroethylene - hybrid
DRIE	deep reactive ion etching
DSP	double side polished
DUV	deep ultraviolet
EBL	electron beam lithography
ECT	eicosanethiol
ELD	electroless deposition
EUV	extreme ultraviolet
FIB	focused ion beam lithography
HCl	hydrochloric acid
HDT	hexadecanethiol
HF	hydrofluoric acid
HMDS	hexamethyl dichloro-silane
h-PDMS	hard poly(dimethylsiloxane)
ICP	inductively coupled plasma
IPA	isopropanol
LPCVD	low pressure chemical vapour deposition
MEMS	microelectromechanical systems
MIMIC	micromolding in capillaries
NA	numerical aperture
NIL	nanoimprint lithography
nTP	nanotransfer printing
ODT	octadecanethiol
PDMS	poly(dimethylsiloxane)
PECVD	plasma enhanced chemical vapour deposition
PMMA	polymethyl metacrylate
PR	photoresist
PS	polystyrene
PU	polyurethane
PVD	physical vapour deposition
RCA	clean for silicon wafers
RF	radio frequency
RIE	reactive ion etching
RM	replica molding (REM)
rpm	rounds per minute
SAM	self assembled monolayer

SAMIM	solvent assisted micromolding
sccm	standard cubic centimeters per minute
SEM	scanning electron microscope
SFIL	step and flash imprint lithography
Si	silicon
SiN	silicon nitride
T_g	glass transition temperature
TMAH	tetramethyl ammonium hydroxide
UV	ultraviolet
q	water contact angle
μCP	microcontact printing
μTM	microtransfer molding
184-PDMS	Sylgard-184 poly(dimethylsiloxane)

Table of Contents

1 Introduction

1.1 Micro- and Nanotechnologies

The trend in electronics fabrication is continuously going towards smaller and smaller structures. Downscaling the size of the components increases their performance and density, lowers the power consumption and the cost. The dimensions in microfabrication are typically 0.1 – 100 µm. The Microfabrication techniques are increasingly being used also outside traditional microelectronics, including microfluidics, microelectromechanical systems (MEMS), such as microsensors, microactuators and micro-optics. Most research in microfabrication is still silicon-based, originating in microelectronics, but new materials and areas of research are also increasing.

Top down nanofabrication is an extension to microfabrication, defined as the process of fabricating structures with the dimensions of 1 – 100 nm. The field of nanotechnologies is growing rapidly, and new ideas are being introduced frequently. When going to nanoscale, entirely new phenomena and properties appear that are not present at bulk materials. These phenomena offer new possibilities and ideas for new devices. [1, 2].

1.2 Conventional Lithography

When the features are miniaturized, the fabrication becomes challenging. The conventional way of patterning structures in microfabrication is lithography. Lithography is a process in which the substrate to be patterned is covered with a layer of radiation-sensitive polymer, a photoresist. The resist is locally exposed to radiation, which modifies the structure of the polymer chain to change its solubility properties. After exposure, the resist is developed in a suitable solution, and the desired pattern is created onto the substrate. Conventional lithography includes photolithography and beam (electron or ion) lithography. [2, 3].

1.2.1 Photolithography

In photolithography, the substrate is covered with a photoresist and a photomask above it, having dark and bright parts, letting the radiation through selected areas. With a positive photoresist, the bright parts of the mask, where the radiation gets through, cause the resist material become soluble in a developer solution, while the dark parts are protected and insoluble and thus remain on the substrate after development in the appropriate solution. In a negative photoresist, the exposed parts become insoluble and unexposed parts are soluble in the developer solution. After development, the pattern of the mask is portrayed by the remaining resist on the substrate. Resist can be used as a mask in subsequent etching or deposition steps. The photolithography process is presented in Figure 1. In Figure 1a, the mask is in proximity contact with the resist, with a gap in between the mask and resist, usually in the range of 3 – 50 μm. The mask can also be in hard contact, with no gap in between, or in projection mode, (Figure 1b) using a lens system that allows for example a 1:4 reduction in feature size. The hard mode offers better resolution than proximity mode, but the masks get damaged in the contact, shortening the mask lifetime. [1, 3 – 5].

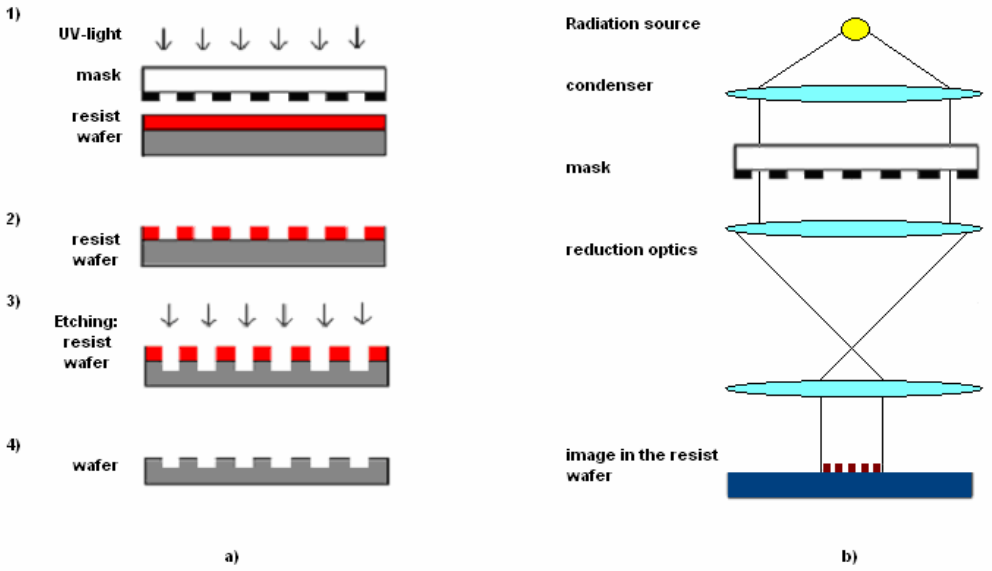

Figure 1. a) Principle of proximity photolithography. a1) A mask is placed on top of the resist-coated wafer, and exposed to UV light, letting the light expose the resist through the holes in the mask. In the next step a2), the resist is developed, in order to remove exposed parts (positive resist) creating a resist pattern on the wafer. a3) the resist pattern can act as a mask in a subsequent etching step, a4) after the removal of resist, wafer has the etched mask pattern. b) the principle of projection lithography with reduction optics in order to reduce the feature size in the wafer. The drawings are not in scale.

In photolithography, the exposing radiation is typically ultraviolet (UV) having the wavelength of 365 – 436 nm. Smaller resolution can be achieved with deep ultraviolet (DUV), wavelength of 193 – 248 nm, or extreme ultraviolet (EUV), wavelength of 10 – 14 nm. In projection mode the size is also decreased using reduction optics. With EUV, the reflective optics have to be specially fabricated, to avoid the problem of absorption in these short wavelengths, as most materials strongly absorb them. Even better resolution can be achieved with X-rays, using high energy and thus short wavelength, around 1 nm. The reduction optics cannot be used with X-ray lithography; it is used in proximity mode. Also mask fabrication is problematic with X-ray lithography. [2, 3].

1.2.1.1 Resolution in Photolithography

In photolithography, the ultimate resolution is defined by the wavelength of the radiation and the masks used. A common approximation for the minimum feature size achieved by proximity photolithography is presented as

$$b_{\min} = \frac{3}{2}\sqrt{\frac{l}{n}\left(g + \frac{d}{2}\right)}, \quad (1)$$

where b_{min} is the minimum feature size, l is the wavelength of the exposing radiation, g is the gap between the resist and mask, d is the resist thickness and n is the refractive index of the resist [2].

With (1), using UV radiation of 365 nm wavelength, 3 μm gap between the mask and the substrate, and a 500 nm thick resist layer with refractive index 1.6 [2] the minimum feature size would be approximately 1.3 μm. Obtaining smaller features with photolithography requires smaller gaps, thinner resist layers and shorter wavelengths, going from UV to deep-UV and extreme-UV radiation.

Resolution in projection lithography is defined by the Rayleigh diffraction:

$$R = \frac{k_1 l}{NA}, \quad (2)$$

where R is the resolution, k_1 is a parameter depending upon the mask and resist used, l is the exposing wavelength and NA numerical aperture of the system [2]. With extreme UV, having a numerical aperture of 0.1, a wavelength of 14 nm and k_1 of 0.7, the minimum resolution is approximately 100 nm [3, 6]. With deep UV, a numerical aperture of 0.7, a wavelength of 193 nm and k_1 of 0.4, the minimum resolution is approximately 110 nm.

1.2.2 Scanning Beam Lithography

Scanning beam lithography is a maskless process, including electron beam lithography (EBL) and focused ion beam lithography (FIB). The sample is covered by an electron or ion sensitive resist layer, a focused beam scans across the sample, and turns on and off according to the data input, exposing the resist point-by-point to produce the image. This is called direct writing. In EBL, the beam consists of electrons; and in FIB the beam consists of ions, typically gallium, (Ga^+). With FIB, direct removal of particles by sputtering the substrate without a resist is also used.

In EBL the resolution is limited by the scattering of electrons, whereas in FIB the ion scattering from the resist and backscattering from the substrate is very low. The major problem in FIB is the damage to samples caused by high energy ions [1]. FIB has higher resist exposure sensitivity than EBL, but throughput of FIB is lower than with EBL because of the much lower velocity of charged ions with respect to electrons when accelerated to comparable energies [3].

With scanning beam techniques, a smaller resolution can be achieved than with photolithography, but the downside is its slowness. Photolithography is a parallel technique, meaning that the whole area is exposed simultaneously, through the mask, scanning beam lithography techniques are serial; point-by point exposure is quite slow, and it is better suitable for research purposes than batch production. EBL is usually used for producing the photomasks for photolithography. [1, 3, 7].

1.2.3 Properties of Conventional Lithography

Microfabrication is done in cleanroom facilities, where air is filtered to control particle contamination, and temperature and humidity are stable. Particles of micrometer-size could destroy a microfabricated device. In semiconductor processes, photolithography is used,

and semiconductors and glass are typically used materials in microfabrication. Organic soft materials cannot always be brought to the cleanroom or used with the cleanroom equipment due to contamination problems. Also some metals such as gold, silver, platinum, nickel, chromium, iron and copper create contamination problems.

With advanced lithography, such as DUV, EUV, EBL or FIB, it is possible to achieve structures in nanoscale, in the resolution of sub 100 nm. This requires high capital cost in equipment. The approximated resolutions, costs and throughputs for various lithography techniques are presented in Table 1. [2, 3, 6].

Table 1. Comparison of nanolithography techniques. All the numbers quoted are approximate and highly configuration dependent. Approximate cost does not include the operating costs such as masks [3].

Lithography Technique	Optical	E-beam (Direct Write)	Focused Ion Beam	EUV
Resolution [nm]	100	20	30	30
Alignment [nm]	30	10	10	10
Throughput [features/s]	10^{10}	10^{4}	$10^{1} - 10^{2}$	10^{11}
Instrument Cost [$]	10^{7}	10^{6}	10^{6}	$\sim 5 \cdot 10^{7}$

1.3 Alternative Lithographies

Micro- and nanostructures are usually patterned by photolithography and etching, based on removal of material, so called top-down approach. These techniques are highly developed and widespread. They have their limitations, however. The patterning of nanoscale dimensions means higher equipment cost with conventional techniques, and going to smaller dimensions requires scanning beam serial techniques, which have a low throughput. The unconventional techniques provide an alternative way to fabricate small structures. Besides the top-down approach, unconventional techniques use also a bottom-up approach, where small components, such as atoms and molecules are put together to form larger systems. They are based on natural chemical, physical and biological processes.

One of these unconventional lithographies is called soft lithography. It is a family of techniques that use organic, soft materials to perform replication and pattern transfer. The term refers to a soft stamp or a soft substrate, such as polymers or self assembled monolayers. Soft lithography techniques are based on molding, replication and pattern transfer. These are alternative lithographic techniques, since instead of radiation exposure they use physical deforming or material transfer to replicate the patterns. Soft lithographic techniques are promising methods for parallel patterning, since they could allow higher throughput, and do not require expensive equipment. The soft lithographic techniques enable the fabrication on non-planar surfaces with a wide range of materials. These are relatively new technologies still at the stage of research. Usually the first step in soft lithography, the master fabrication needs the use of conventional lithography, so it cannot be done completely without cleanroom and high-cost equipment. High-cost, high-resolution, slow-throughput equipment can be used in the master fabrication, and low-cost soft lithography in replication of the features of the master. [1, 8].

1.4 Purpose of This Work

The purpose of this work was to fabricate an array of gold dots onto a substrate. In chapter 1, a number of different micro- and nanofabrication techniques are reviewed. The methods discussed are soft lithography techniques, using molding, printing and embossing as methods to fabricate patterns with small dimensions. In chapter 2, different soft lithographic techniques are introduced, in chapter 3, some important materials for soft lithography are presented. Chapter 4 focuses on the experimental procedure of microcontact printing and transfer printing for gold dot array fabrication. The tests made with different master designs and results are presented in chapter 5, followed by the conclusions in chapter 6.

2 Soft Lithographic Techniques

Soft lithography is based on pattern transfer using a mold that is deforming or patterning the substrate material. Most of the soft lithographic techniques use mold formed of a master template. The fabrication of an elastomeric mold is presented in Figure 2. The mold replicates the inverse of master features, and it can be used in turn to deform or pattern the next material.

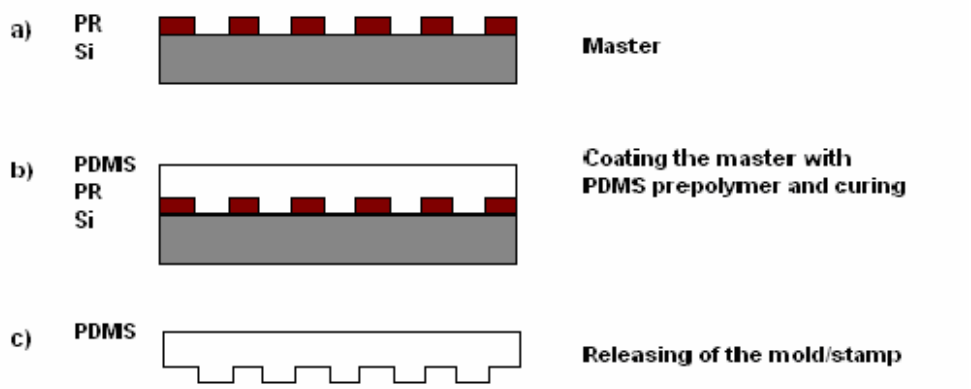

Figure 2. The principle of fabrication of polymer stamp or mold for soft lithography.

The process begins with the master fabrication, usually made of silicon having topographical features like trenches and ridges as shown in Figure 2a. The mold is fabricated by casting the liquid precursor, usually a prepolymer mixture into the master (Figure 2b). The mold is then cured to make it solid, and removed from the master (Figure 2c). This mold will then be used in subsequent patterning steps. The fabrication of the master is usually done with photolithography or when very small features are needed, by electron beam lithography. The master has to have smooth sidewalls and bottom surfaces and it can be coated with a release layer to ease the removal of the mold. In master fabrication soft lithography is not independent of cleanroom facilities and high-cost equipment. Its strength is rather in replication: once the master is created with the expensive or low-throughput equipment, it can be used multiple times, with no need to

have the slow EBL step done each time a pattern is created, thus overcoming the limits of slow throughput with scanning beam lithography and making soft lithography an attractive alternative in nanoscale patterning. Variety of materials can be used, and some of these techniques allow the patterning of curved non-planar surfaces and the replication of three-dimensional structures.

Soft lithography includes a wide variety of techniques. Here, they are organized as proposed by Gates et al. [6], in three categories: replica molding, embossing and printing, which all include sub-categories. The categories used in this work are presented in Figure 3. The nomenclature in this area is not fully established, and definitions might vary in different references, especially the difference between embossing and molding is not always clear. [6, 8].

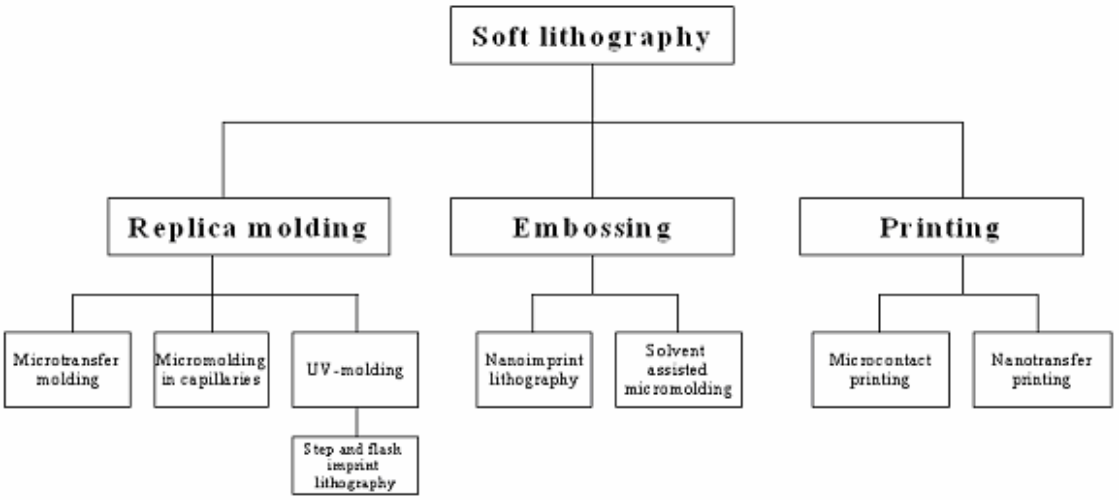

Figure 3. Soft lithographic techniques divided into groups of replica molding, embossing and printing, each having sub-groups of techniques.

2.1 Replica Molding

Replica molding (RM, REM) includes transfer of topographical features from a rigid master or soft mold, referred here as the master. The features are transferred by solidifying a liquid prepolymer mixture in contact with a master. The liquid prepolymer conforms to

the form of the master and exposure to UV radiation or suitable temperature induces the crosslinking, making the polymer solid. Removal of the master creates an inverse replica, referred to as the mold. The process described in Chapter 2, Figure 2 is the simplest form of replica molding. The polymer mold is often made of poly(dimethylsiloxane) (PDMS). The soft polymer mold can be used as a master in the next step, to mold another liquid prepolymer, such as polyurethane (PU) [1]. This is depicted in Figure 4. A microstructure fabricated by replica molding is shown in Figure 5.

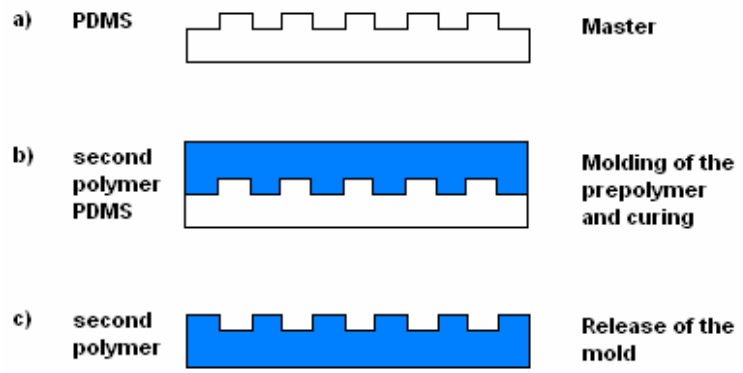

Figure 4. Replica molding: casting the prepolymer mixture into a PDMS master and crosslinking it then removing the master, thus fabricating the stamp or mold [6].

Replica molding with a soft elastomeric poly(dimethylsiloxane) PDMS mold includes microtransfer molding (μTM) and micromolding in capillaries (MIMIC). MIMIC and μTM have the same principle as basic replica molding in Figure 4, but they create the polymer structure onto another solid substrate. A structure created by replica molding of polyurethane is shown in Figure 5. The use of a soft PDMS mold as a master in molding has advantages, such as low surface energy of the PDMS mold, allowing the release easily [1]. The permeability to gas of PDMS allows the air bubbles diffuse through, not causing problems as in hard master, where the bubbles get trapped. Also, the soft master has the ability to mold against non-planar surfaces unlike a hard master.

Replica molding with a rigid master such as silicon or quartz includes UV-molding. One of the UV-molding techniques is step and flash imprint lithography (SFIL)™. Hard mold has also its advantages. Master made of silicon or quartz retains the features with minimal deformation with the pressures during soft lithographic fabrication processes, it is thermally

stable at high temperatures and chemically inert. Surface fouling can be a problem, dependent on the surface free energies of the master and the polymer to be mold [7]. A coating layer can be used with a hard master to ease the release [6, 7 – 9].

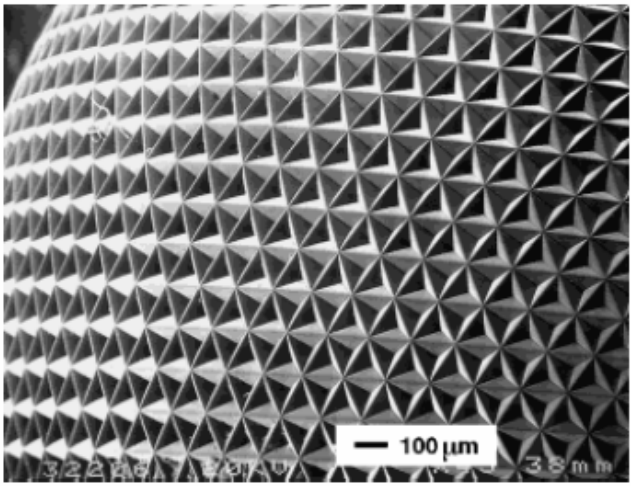

Figure 5. A scanning electron micrograph of polyurethane with patterned microstructures on its surface that was formed by replica molding against a stretched PDMS mold [8].

2.1.1 Microtransfer Molding

In microtransfer molding (µTM), the elastomeric poly(dimethylsiloxane) (PDMS) mold is used as a master, and it is fabricated as presented in Figure 2. The µTM process is presented in Figure 6. A liquid prepolymer, such as polyurethane (PU) or thermally curable epoxy [8] fills the recessed regions of the PDMS master. The excess prepolymer is removed; the prepolymer is placed in contact with a rigid substrate and cured. After curing, the PDMS master is removed. The film of polymer that remains between the features on top of the substrate is called scum and can be removed using reactive ion etching (RIE), if the features need to be separated. This method can create three-dimensional structures and pattern both planar and curved substrates. Repeating the process can build multilayer structures. A structure fabricated by µTM is shown in Figure 7. Since the PDMS mold is permeable to gas, the air bubbles do not get trapped in the mold. [6, 8].

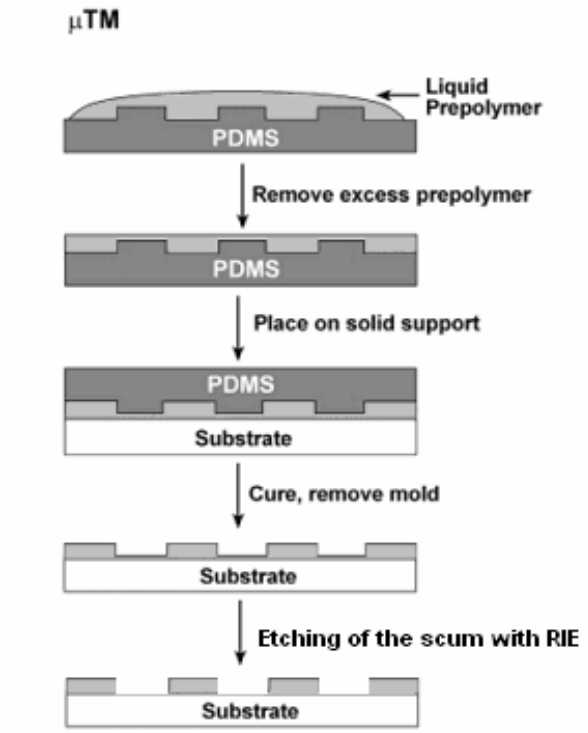

Figure 6. Microtransfer molding. Modified from [6].

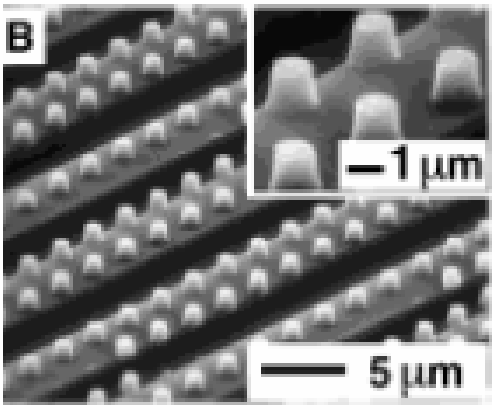

Figure 7. Two-layered structure of isolated microstructures of epoxy on lines of epoxy supported on a glass slide [8].

2.1.2 Micromolding in Capillaries

Micromolding in capillaries (MIMIC) resembles microtransfer molding, but in this technique the soft PDMS master has a microchannel structure. The PDMS master is placed

onto a substrate, having the channels faced down. The liquid prepolymer is placed next to the open ends of the channels, and the capillary forces pull the liquid to fill the channels. The liquid is crosslinked, and the PDMS master removed. The process is shown in Figure 8. In this technique no scum is created, the structures are formed in a single step. A structure made by MIMIC is shown in Figure 9. The structures fabricated with this technique are obviously limited to channels. Since the rate of filling of the capillary is proportional to the cross section of the channel, the slow filling of small capillaries might limit the feature size. [8, 10].

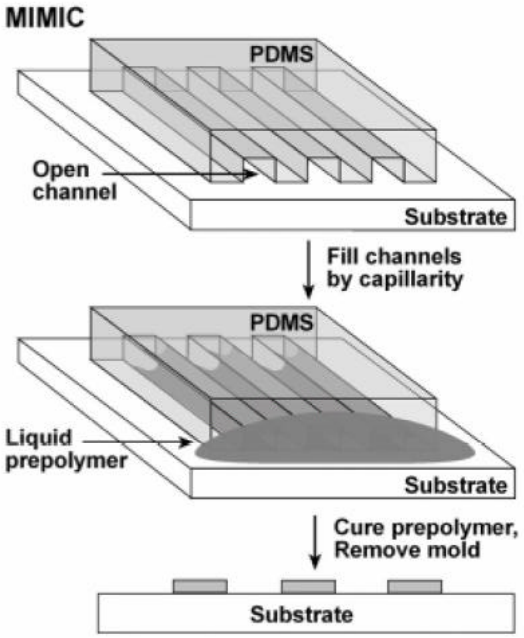

Figure 8. Micromolding in capillaries [6].

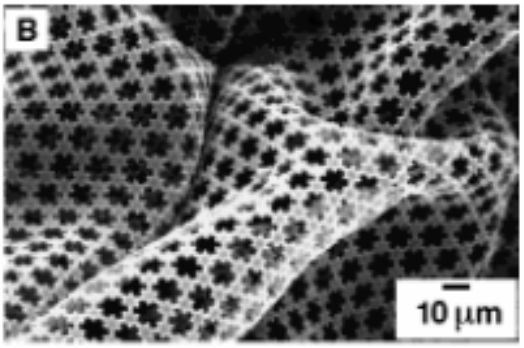

Figure 9. Polymeric microstructures of polyurethane fabricated by MIMIC [8].

2.1.3 UV-Molding

Ultraviolet-molding (UV-molding) technique differs from the two RM techniques presented above in the fact that it usually uses a rigid master, even though a soft PDMS master can be used also. The curing in MIMIC and μTM is usually done with a rise in temperature, but UV-molding uses UV radiation, and thus a UV-curable prepolymer that is crosslinked by exposing it to UV radiation. The prepolymer is molded onto a master and a substrate is placed on top of it, resembling μTM technique. In Figure 10, a process is presented, in which the UV radiation is exposed to the prepolymer mixture through a transparent substrate. Another option is to use a transparent master, and expose the prepolymer through the master.

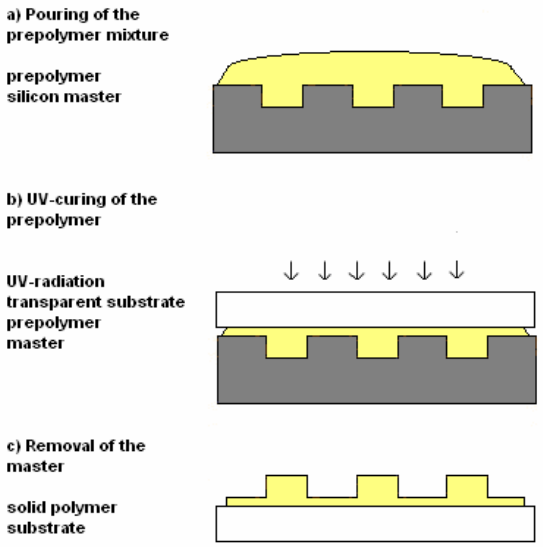

Figure 10. UV-molding of a UV-curable polymer through a transparent substrate, such as glass or quartz [10].

2.1.3.1 Step and Flash Imprint Lithography™

Step and flash imprint lithography™ (SFIL™) is a special version of UV-molding. It is a registered trademark of the Willson group [11]. SFIL™ replicates topography of a rigid transparent master using a photocurable prepolymer solution, such as photocurable polyurethane (PU) or organosilicon as the material to be molded. A low-viscosity liquid

fills the spaces of the transparent master, usually made of quartz. Exposing the prepolymer to UV light causes the crosslinking and the master is removed. The residual layer that is left connecting the polymer features can be removed by RIE. The technique is presented in Figure 11.

SFIL does not suffer the thermal mismatch induced by thermal expansion. The pressure is also very low, so pressure induced deformations are also minimal, allowing the use of brittle substrates. High aspect ratios are also possible. It also is a very fast technique compared with the other soft lithographic techniques, only 5 minutes per cycle[1]. The transparent master allows the features to be optically aligned to the underlying layer. The fabrication on non-planar substrates is however difficult with SFIL. Air bubbles can be trapped between the master and the polymer. The fidelity and stability for multilayer structures are yet not optimal. Surface fouling of the pattern is however dependent on the surface free energies of the mold and the polymer. A release layer reduces the surface free energy of the mold and minimizes adhesion of crosslinked polymer to the master. If the release layer fails, the molded polymer can adhere to the master and foul its surface or break its features [7]. [6, 12].

[1] In optical lithography the exposure can be as fast as 1 second.

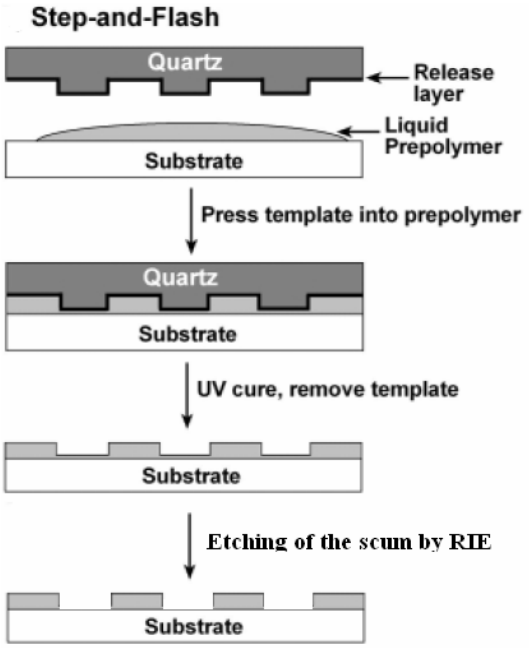

Figure 11. Step and flash imprint lithography. Modified from [6].

2.2 Embossing (Imprinting)

Embossing is the process of imprinting a pattern into an initially flat solid surface by pressing a mold and softening the surface. The difference between replica molding and embossing techniques is the material to be molded: in embossing it is a solid film, in replica molding a liquid precursor. The polymer is embossed thermally, with pressure, or with solvent assistance. Embossing can use a rigid or a soft mold. Embossing techniques presented here are nanoimprint lithography, which uses a rigid master and solvent assisted micromolding, which uses a soft mold as a master. [6].

2.2.1 Nanoimprint Lithography

Nanoimprint lithography (NIL), developed by Chou et al. [13], also called hot embossing, uses usually a hard rigid master to physically deform a solid polymer film that is on a rigid substrate surface. The polymer on a substrate surface is heated above its glass transition

temperature (T_g), and the master is pressed against it. The polymer is deformed filling the voids in the master, then it is cooled below T_g, and the master is removed revealing a pattern that is the inverse of the master. The principle of NIL is presented in Figure 12. In Figure 13, structures made in a polymethyl metacrylate (PMMA) film by NIL are shown. Another example is to emboss is polystyrene (PS) with a soft PDMS master [14].

NIL has a problem with the lifetime of the master, because the heating and cooling cycles and pressures it experiences, cause ageing [7]. To prevent thermal cycling related problems, another way to emboss a polymer is to apply a high pressure in a room temperature. When a rigid master is used, a release layer is usually used and the problem of the trapped air bubbles exists [6].

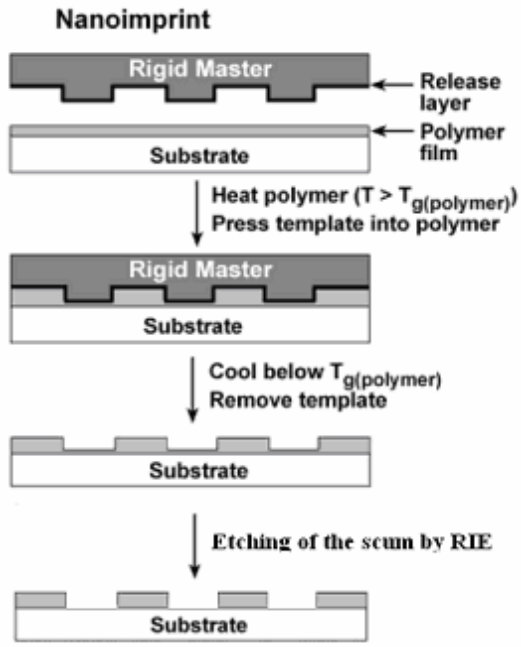

Figure 12. Nanoimprint lithography. Modified from [6].

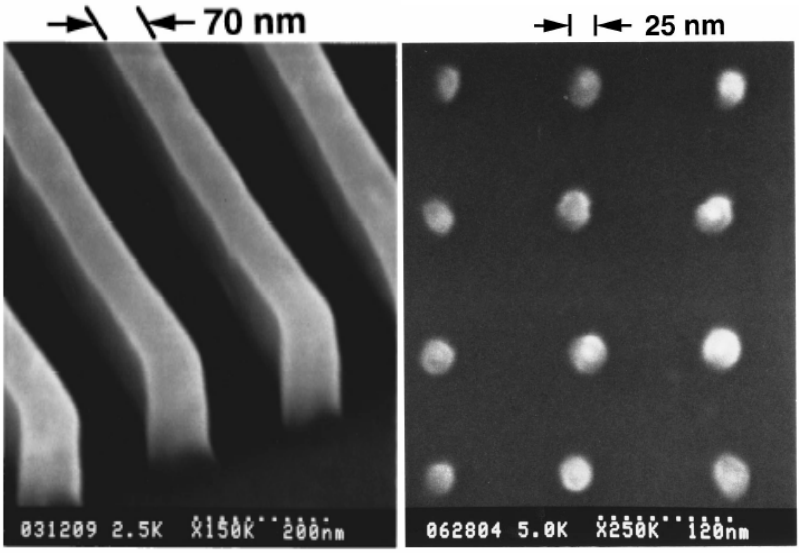

Figure 13. Scanning electron micrographs of (on the left side) lines formed into a PMMA film by imprint. The lines are 70 nm wide and 200 nm tall, have a high aspect ratio, a surface roughness less than 3 nm, and nearly perfect 90° corners On the right side 25 nm diameter and 120 nm period metal dots fabricated by imprint lithography and a lift-off process. [13, 15].

2.2.2 Solvent Assisted Micromolding

Solvent assisted micromolding (SAMIM) uses a soft mold and an appropriate solvent to emboss a polymer film. The solvent softens the polymer so that it can be deformed by the soft mold, and solvent is then evaporated through the mold, usually PDMS. After the solvent has evaporated, the mold is removed and a patterned relief structure of the mold remains. This is presented in Figure 14. A wide variety of organic polymers can be embossed, such as polystyrene and polymethyl metacrylate (PMMA). The advantages of elastomeric mold are the permeability to air bubbles and its ability to conform to non-planar surfaces. Release layers are often not needed. SAMIM is self-cleaning, dust particles on the surface of the stamp tend to remain in the molded polymer so the mold is cleaned by each cycle [1]. On the downside, some solvents can swell PDMS. A thin layer, typically 10 nm, of polymer is left between the features. This can be removed by RIE. [6].

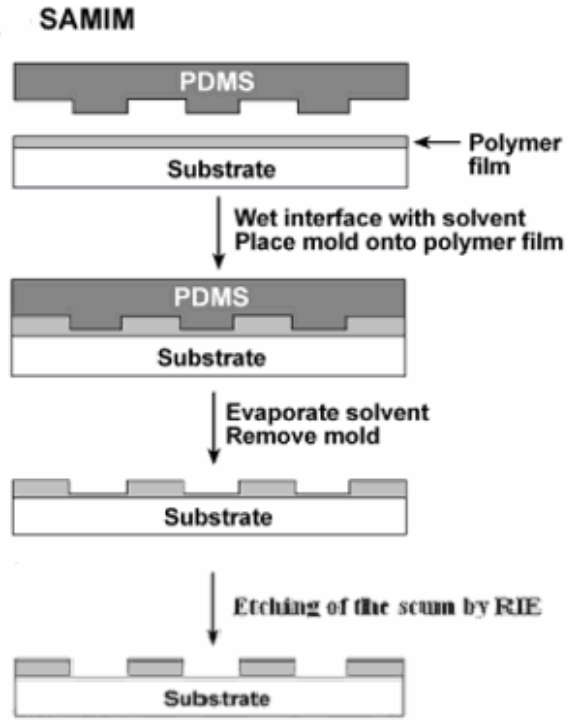

Figure 14. Solvent assisted micromolding. Modified from [6].

2.3 Printing

Printing includes material transfer from the mold onto the substrate.

2.3.1 Microcontact Printing

Microcontact printing (μCP) is a technique in which a patterned elastomeric stamp is used to transfer a surface pattern onto a substrate. The stamp is inked with a material to be transferred, and by a conformal contact between the protruding features of the stamp and the solid substrate; the material is transferred from the stamp to the substrate, creating the desired pattern. The principle of microcontact printing is presented in Figure 15.

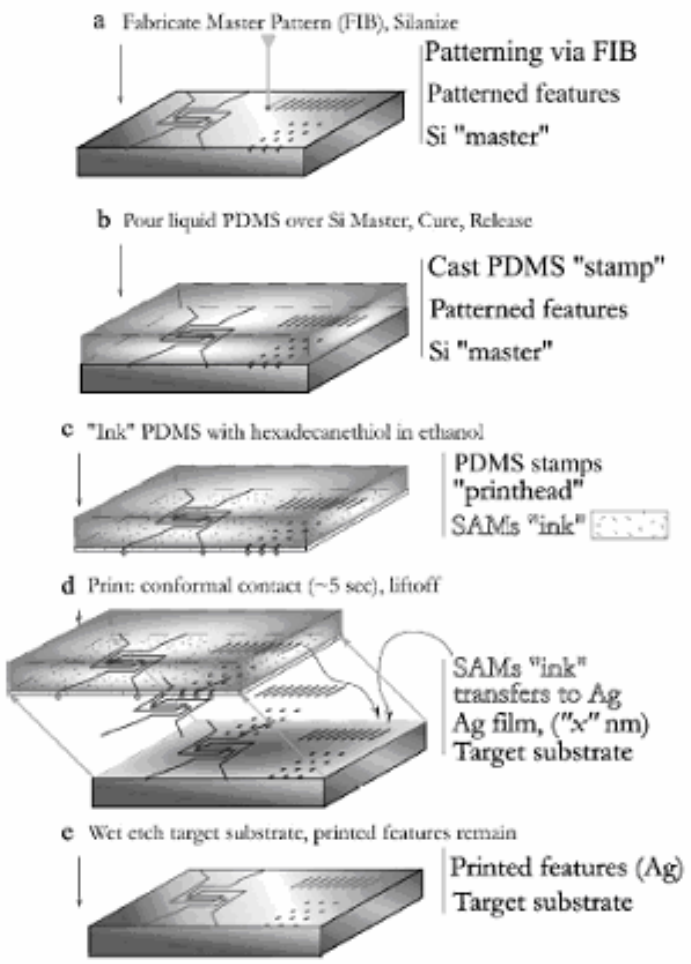

Figure 15. The principle of microcontact printing [16].

The master is typically made of silicon and can be fabricated by photolithography, or if features below 1 µm are needed, by electron beam lithography. The stamp material is usually PDMS, and fabricated as described in chapter 2.1. The stamp is inked with an appropriate solution, and placed in contact with the substrate to be printed. The stamp makes a conformal contact with the substrate, so that only the protruding features of the stamp touch the surface, and in an ideal case the ink is transferred only at these areas. The pattern of the initial master is thus transferred onto the substrate. The best-known example of microcontact printing is the printing of self assembled monolayer (SAM) of alkanethiolates onto the areas of a film of noble and near-noble metals. Other examples are silanes on oxides or alkyl phosphates on metal oxides and proteins on silicon or glass [17, 18]. The convenience of microcontact printing is that the same stamp can be used multiple

times, and the same master can be used to produce several stamps. The material of the stamp needs to be elastomeric, to ensure a conformal contact between the substrate and the stamp, as shown in Figure 16.

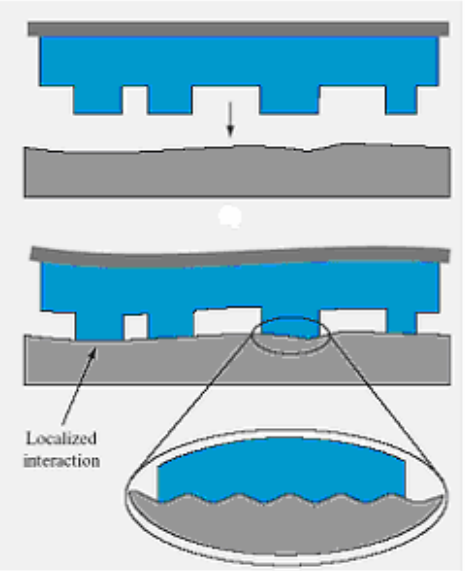

Figure 16. Conformal contact between an elastomeric stamp and the substrate surface's irregularities [20].

The microcontact printed patterned SAMs can be used as etch resists or catalytic seed pattern for electroless deposition (ELD) of metal patterns [18, 19], as presented in Figure 17. The printed pattern can change the surface properties of the substrate and influence the wetting and adhesion properties of the surface. [18, 20].

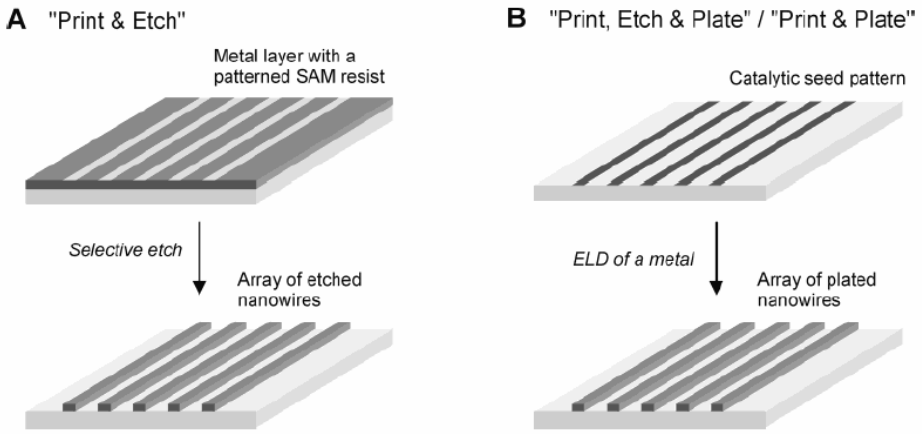

Figure 17. Two methods of fabricating metal structures using microcontact printing. In the first method (A) a resist is printed on a metal film and the pattern is transferred by etching. In the second one (B) a catalytic seed pattern is printed onto a substrate and a electroless deposition of a metal will occur onto the patterned areas [18].

2.3.2 Nanotransfer Printing

Nanotransfer printing (nTP) is an additive technique of printing micro- and nanoscale features onto a substrate, without etching steps. Solid layer of material, typically metal, is used as 'ink' in this method. A patterned hard or elastomeric stamp is coated with metal and it is transferred from the protruding features of the stamp. The substrate to be printed has an adhesion layer on its surface, designed to promote the adhesive bonding of the metal. The surface chemistries are used as interfacial glues and release layers to control the transfer of solid material coatings from the stamp to a substrate [21]. The strength of adhesion between the metal and the stamp is smaller than that of the substrate and metal during contact [22, 23]. The principle of nanotransfer printing is presented in Figure 18.

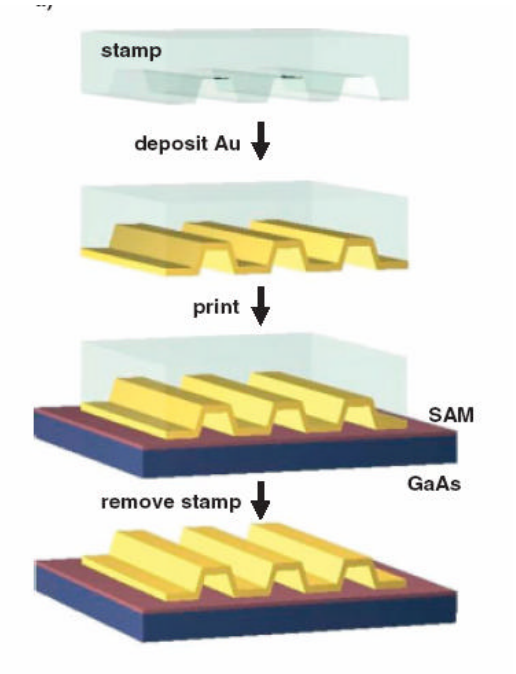

Figure 18. The principle of nanotransfer printing [21].

One possible combination of materials is a layer of gold on the stamp and the substrate coated with a dithiol SAM [21]. In this case the exposed thiol group will covalently bound to the gold layer in the regions of contact. Loo et al. [24] have presented a process in which a substrate with terminal hydroxyl groups is used to create patterns of gold. Other examples are a gallium arsenide (GaAs) substrate, treated with 1,8-octanedithiol and a transfer of copper [25]. Structures created by nanotransfer printing are presented in Figure 19. Nanotransfer printing does not suffer the problem of the diffusion of the SAMs. [24].

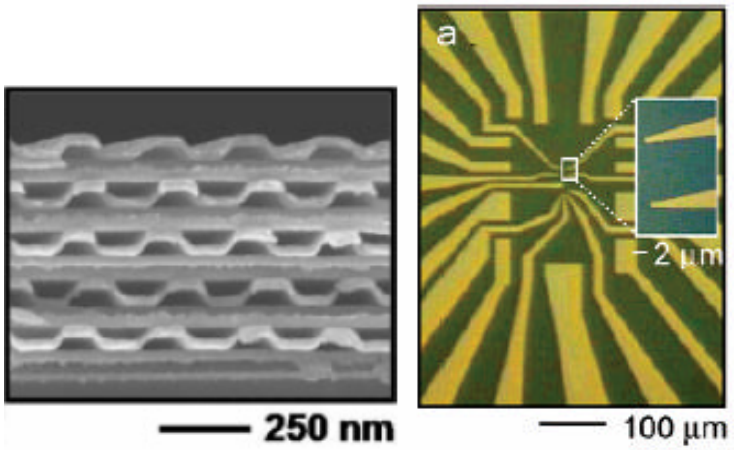

Figure 19. Optical microscope images of gold patterns formed by nanotransfer printing [21, 23].

3 Materials for Soft Lithography

In this chapter, some materials that are widely used in soft lithography are presented.

3.1 Poly(dimethylsiloxane) PDMS

In soft lithography, many of the techniques use an elastomeric stamp or mold. Elastomers are crosslinked amorphous polymers that are used at temperatures above their glass transition temperature, T_g. Above the glass transition temperature, molecules gain thermal energy that enables them to move in a coordinated manner, making the elastomers rubbery, soft and flexible. The most widely used elastomer material for soft lithography is poly(dimethylsiloxane) (PDMS). The chemical structure of PDMS is presented in Figure 20.

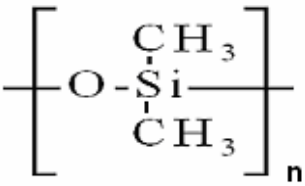

Figure 20. The structure of poly(dimethylsiloxane) (PDMS).

PDMS consists of an inorganic siloxane backbone and organic methyl groups attached to it. PDMS has many attractive properties, as presented in Table 2. It is a flexible elastomer that can be used in a wide temperature range, it is optically transparent, biocompatible, inert and non-toxic and resistant to many chemicals. It is non-flammable and gas-permeable. Thermally and electrically it is insulating. The low surface energy of PDMS allows its release easily from templates and structures. [6, 9, 26 –31]. Curing of PDMS can be done in room temperature, or rapid heat curing in temperatures of 60 – 120°C [28]. In curing, no solvents are evaporated or cure by-products produced. In the literature PDMS is sometimes referred as 184-PDMS due to its commercial name Sylgard-184 [28].

Table 2. Properties of PDMS. [28]

The properties of PDMS after curing	
Stability temperatures	–50°C to +200°C
Durometer hardness, Shore A	50
Tensile strength	7.1 MPa
Elongation at break	1.4
Young's modulus (tensile modulus)	in the range of 1 – 5 MPa [6, 32][2]
Surface energy	low, approximately 21.6 mJ/ m^2 [6, 7]
Linear coefficient of thermal expansion	310 ppm/°C
Hydrophobicity	hydrophobic, water contact angle 90 – 120 [32]
Permeability to gases	passes gases easily
Optical properties	optically transparent down to ~300 nm
Viscosity (prior to curing)	medium viscosity, at 23ºC immediately after mixing: 4000 mPa·s
Elastic modulus	1.8 MPa [33]
Compressibility	high, 2 N/ mm^2 [34]
Shear modulus	$\leq$ 1 GPa [36]
Work of adhesion	10^{-7} J/mm^2 [35]

3.1.1 Problems with 184-PDMS

PDMS has some problems, however. PDMS has appropriate mechanical properties to achieve conformal contact, but it is incapable of printing accurate sub micrometer patterns [35]. Also, due to its softness and mechanical flexibility, replication of features of high aspect ratio have a tendency to pair together, as depicted in Figure 21. Also, distortion of nanoscale features is limiting the use of PDMS in small dimensions. One cause for distortion is polymer shrinkage during curing. Distortion can also occur due to adhesive

[2] The Young's modulus of PDMS has been given different values in the references. According to ref. [32] it varies with the mixing ratio from $3.6 \cdot 10^5$ to $8.68 \cdot 10^5$ Pa, in ref. [31] 1 MPa, in ref [20] 2.5 MPa, tensile modulus in ref. [6] 4.77 MPa.

forces during separation of the master and stamp. PDMS has a low surface energy, so usually it does not adhere to the master. [6].

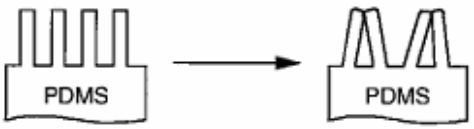

Figure 21. Problems with PDMS stamp fabrication: pairing of high aspect ratio structures. Modified from [8].

The physical properties of 184-PDMS limit the resolution when used in the nanometer regime. For example, tall and narrow features of surface relief are unstable to mechanical collapse [33]. The low elastic modulus for 184-PDMS (1.8 MPa) [33] and high compressibility [6] make the replication of nanoscale features with high aspect ratios difficult using soft lithography. Structures smaller than 1 μm tend to merge or collapse during printing and inking. Structures tend to deform upon release from the master because of surface tension [35], and the perfectly sharp corners in the silicon master cannot be replicated to PDMS mold because after release, surface tension forces will reform the sharp corners into smooth and rounded equilibrium shapes. According to the calculations by Hui et al. [36] the lower limit for the radius of curvature for corners in PDMS structures is in the order of 50 nm. [34 – 36].

3.1.2 Surface Modification of PDMS

The surface of PDMS is hydrophobic due to the methyl groups ($-CH_3$). Its surface can be transformed hydrophilic, by for example plasma oxidizing treatment, which creates silanol groups ($Si-OH$) and removes methyl groups. Plasma-treated surfaces can be kept hydrophilic by keeping them in contact with water, but in air surface rearrangements bring new hydrophobic groups in order to decrease the surface free energy and surface deoxidizes in less than an hour. [9, 29].

3.1.3 Hard-PDMS

The possibility to print high resolution features has been studied by Schmid and Michel [35], who have developed a commercially available polymer having a higher modulus (10 – 12 MPa [18]) and surface hardness to solve the problems associated with the 184-PDMS in printing sub micrometer sized patterns. This material is called hard-PDMS (h-PDMS). It was specially developed for the application of microcontact printing of alkanethiolates on metals.

Greater modulus however leads to a brittle material that does not have the ability to conform to substrate. Composite bilayer stamp structures that use a thin layer of the h-PDMS with a backing of 184-PDMS combine some of the attractive features of these two materials for certain purposes: to have a rigid layer to achieve high resolution in pattern transfer and to have a flexible support to enable conformal contact with a substrate [34].

3.2 Self Assembled Monolayers

Self assembled monolayers (SAMs) are thin films with a thickness of a single molecular layer. The SAM system has a surface-active head group that attaches to its corresponding substrate spontaneously via a chemisorption process. The most-studied example of ordered SAMs is alkanethiol-gold system, the formation of highly ordered alkanethiolates on gold. Other examples of SAM systems are alkanethiols on silver and copper, and alkylsiloxanes on hydroxyl-terminated surfaces, such as silicon dioxide, or glass. The monolayer forms spontaneously, and is at or close to thermodynamic equilibrium. SAMs are highly ordered, they reject defects and tend to be self-healing and stable. SAMs of alkanethiolates on gold become disordered or decompose at elevated temperatures around 100°C. [37].

3.2.1 Thiol-Gold System

A straight chained thiol molecule has a structure denoted as $SH(CH_2)_nX$, in which X presents one head group, the other head group is a thiol group $–SH$, and the body consists

of an alkyl chain, $(CH_2)_n$. The head group, X can be for example a methyl group, $-CH_3$, carboxyl group, $-COOH$ or hydroxyl group, $-OH$. The chemical surface properties can be tailored by using SAMs with different head groups. Alkanethiols have a terminal methyl group $(-CH_3)$, making its surface hydrophobic. The structure of alkanethiolate SAM on gold surface is presented in Figure 22.

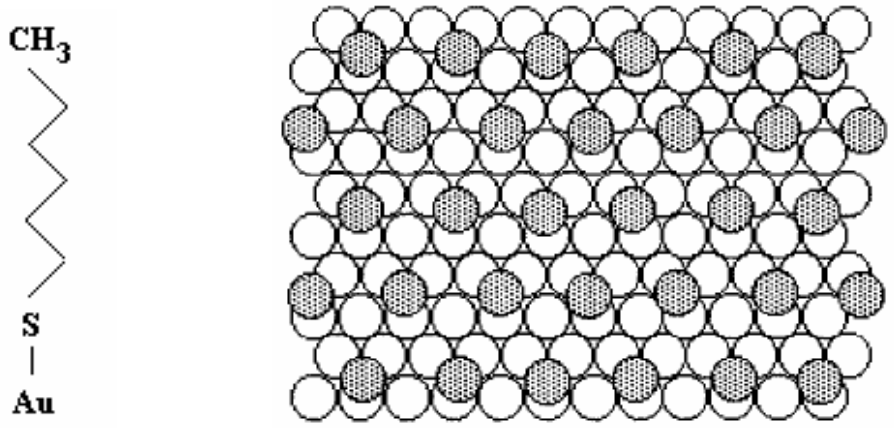

Figure 22. Alkanethiolates on gold. On the left, the structure of an alkanethiolate molecule on gold surface, the bonding between sulphur and gold, the alkane chain denoted by lines and the methyl end group at the surface. On the right, a top view of the hexagonally packed structure of alkanethiolates on Au(111). The open circles denote gold atoms and the shaded circles denote sulphur atoms. Modified from [38].

In the thiol-gold system, the sulphur atom in the thiol group forms a bond with the gold atom, creating a thiolate molecule onto the gold surface. The exact details of the bond formation are not yet fully known. The reaction that is believed to take place is presented as

$$X(CH_2)_nSH + Au^0 \rightarrow X(CH_2)_nS^{-}Au^I + \tfrac{1}{2}H_2, \qquad (3)$$

where X denotes an end group such as methyl group [8].

The type of bond that forms in the case of equation 3 is a coordinate covalent bond. It is formed by coordination of a ligand by a donating two electrons to a metal [3]. Ulman [38] describes the formation of alkanethiolates on gold as an oxidative addition of the $S-H$ bond to the gold surface, followed by a reductive elimination of the hydrogen. The thickness of an alkanethiolate SAM on gold is typically 1 – 3 nm, and can be controlled by

the number of the carbon atoms in the alkyl chain. Sulphur atoms of long chain alkanethiolates form a hexagonally packed structure on Au(111) surface, as is depicted in Figure 22. They tilt at an angle of approximately 30° from the normal of the surface to maximize the favorable van der Waals interactions between adjacent chains, creating an order similar to crystal order in solid materials. The ordered structure is presented in Figure 23. [5, 37, 39].

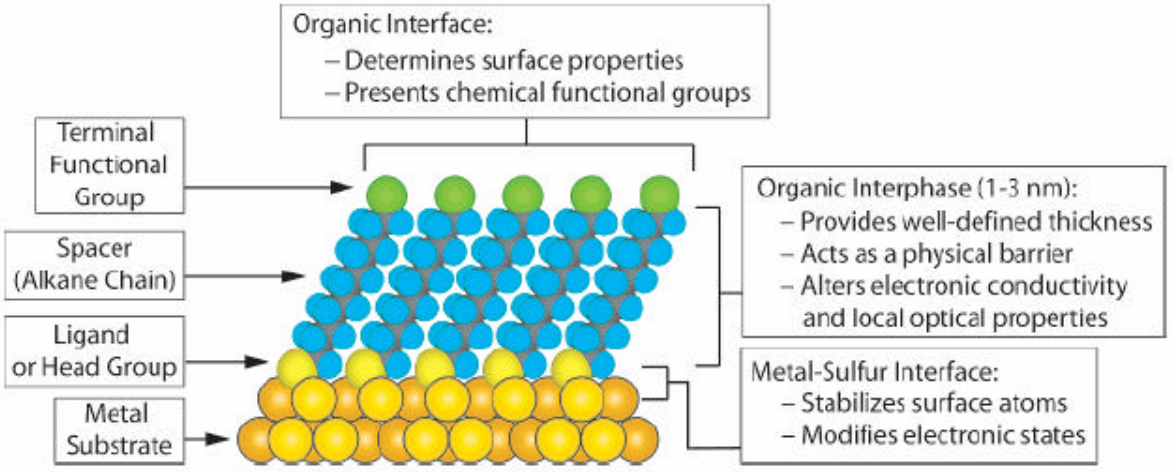

Figure 23. Ideal structure self assembled monolayers of alkanethiolates on gold [39].

3.2.2 Alkanethiol Diffusion in Microcontact Printing

Alkanethiolate SAMs can be fabricated onto gold selectively by microcontact printing, as described in chapter 2.3.1. For this purpose, the alkanethiol diffusion on the stamp presents a problem, as shown in Figure 24. The diffusion of the thiols cause distortion of the patterns and determines the quality of the microcontact printed pattern [17]. The molecular weight of the alkanethiol has an effect on the diffusion properties. Eicosanethiol is an alkanethiol, having the chemical formula $C_{20}H_{41}SH$. Terminal group of $-CH_3$ makes its surface hydrophobic. Eicosanethiol is a long chain alkanethiol, n=19, and it is less diffusive than the shorter chain alkanethiols, such as octadecanethiol (ODT, n=17) and hexadecanethiol (HDT, n=15) [40]. Low concentration of the solution and high molecular weight of the alkanethiol reduce the diffusion [41]. On the other hand, the stress at

monolayer film increases linearly with the length of the alkyl chain of the molecule [42]. Eicosanethiol is a good compromise between diffusion properties and etch mask properties [31].

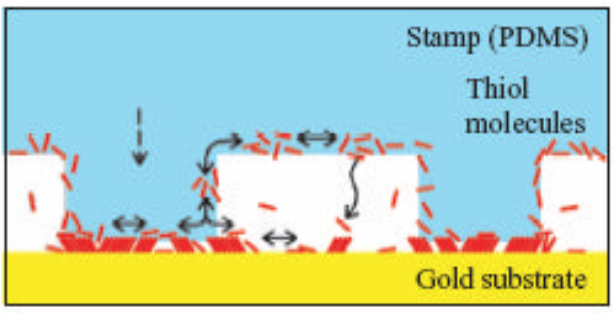

Figure 24. The diffusion of alkanethiols during printing [20].

4 Materials and Methods

In this work, microcontact printing technique was used for the purpose of fabricating a regular array of gold dots onto a substrate surface. Some experiments were also done using transfer printing technique. Different master designs have been tested for their suitability to print arrays of dots.

The procedure of microcontact printing is presented in chapters 4.1 – 4.5. First, the different master designs and their fabrication is presented in chapter 4.1. The procedure of stamp fabrication is described in chapter 4.2, and substrate preparation in chapter 4.3, followed by the printing procedure in chapter 4.4 and finally etching in chapter 4.5.

The procedure for the transfer printing experiments is presented in chapters 4.6 – 4.10. Beginning with the explanation of the procedure in chapter 4.6, master fabrication is described in chapter 4.7, substrate preparation in chapter 4.8, gold coating of the stamp in chapter 4.9 and finally printing in chapter 4.10.

4.1 Master Fabrication for Microcontact Printing

Three types of masters were tested in this work. The fabrication of the masters is described in detail in the following chapters. In chapter 4.1.1, inverted pyramid master fabrication is described. In 4.1.2, a low aspect ratio photoresist master fabrication and in chapter 4.1.3 a high aspect ratio DRIE silicon master fabrication is presented.

4.1.1 Inverted Pyramid Master Fabrication for Microcontact Printing

The fabrication of the inverted pyramid master for microcontact printing is presented in Figure 25.

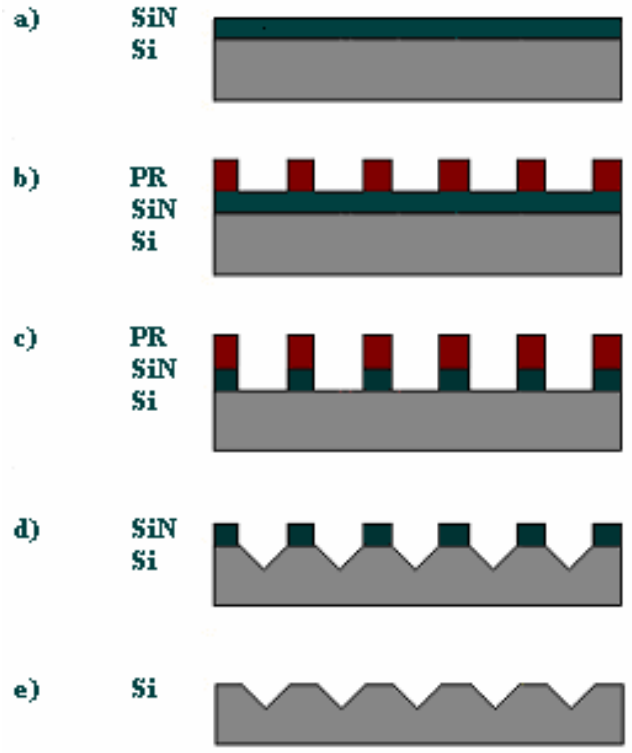

Figure 25. Inverted pyramid master fabrication: a) nitride deposition b) resist application and patterning with photolithography c) etching the pattern into the nitride d) resist removal and anisotropic etching of silicon e) etching of the nitride layer.

The idea of this design is to fabricate masters with inverted pyramid shaped holes, so that the very tip of the molded PDMS pyramid would be as sharp and small as possible. The patterning is done with photolithography followed by anisotropic etching of silicon to produce inverted pyramid shapes. The fabrication steps are explained in the following chapters.

4.1.1.1 Plasma Enhanced Chemical Vapour Deposition of Nitride

Standard (100) crystal orientation, 4-inch RCA-cleaned silicon wafers (*Okmetic Ltd, Finland*) with resistivities typically of 1–12 Ω cm, and thicknesses of 380 – 500 µm were used. A deposition of silicon nitride (Si_3N_4) film onto the wafer was done with a plasma enhanced chemical vapor deposition (PECVD) (*Oxford 80+, Oxford Instruments Plasma Technology, UK*). The composition of a PECVD nitride is not ideally stoichiometric Si_3N_4, but it is usually SiN_x with $x \approx 0.8$ [2]. In PECVD, the source materials are gases, and induced by plasma, they decompose and react to deposit a film on the substrate. The gases used were 380 standard cubic centimeters per minute (sccm) of nitrogen (N_2), 20 sccm of silane (SiH_4) and 30 sccm of ammonia (NH_3). The deposition time was 10 minutes and the resulting film thickness was typically around 250 nm, measured by ellipsometry. The parameters used in nitride deposition are presented in Table 3.

Table 3. Parameters in the nitride deposition with PECVD.

N_2	380 sccm
SiH_4	20 sccm
NH_3	30 sccm
Temperature	300°C
Pressure	1000 mtorr
RF-power	20 W

4.1.1.2 Lithography

A standard photolithography process was performed to pattern the resist with an array of holes. The first step was a prebake to remove moisture, followed by priming in 1,1,1,3,3,3-hexamethyl disilazane (HMDS, $(H_3C)_3$-Si-NH-Si-$(CH_3)_3$) vapour to make the surface hydrophobic and prevent moisture condensation, improving the adhesion of the resist. Then, a positive photoresist (*AZ5214E, Clariant, Germany*) was spin-coated onto the wafers. The spinning speed was 4000 rounds per minute (rpm) for 25 seconds. This results

in a 1.5 µm layer of resist. Then, a soft bake was done to remove the remaining solvent in the resist, followed by the exposure through a chromium glass mask with a mask aligner *Electron Visions AL6-2* (*Electronic Visions, Inc., Phoenix, AZ, USA*), using a hard contact between the mask and substrate. The exposure time was typically 4 seconds. The parameters used for photolithography are presented in Table 4.

Table 4. The process of lithography.

1.) Prebake	120°C, 10 min
2.) HMDS priming	10 min
3.) Resist spinning	4000 rpm, 25 sec
4.) Soft bake	95°C, 20 min
5.) Exposure	Hard contact, 350 W, 350 nm, 4 s
6.) Development	NaOH-based solution, 60 s
7.) Hard bake	120°C, 20 min

Two different mask designs were used, as presented in Figure 26, a mask with 10 µm squares, creating square holes of 10 µm diameter with 2 µm spacing on the resist, and a mask with 2 µm holes, creating 2 µm round holes with spacing of 2 µm onto the resist.

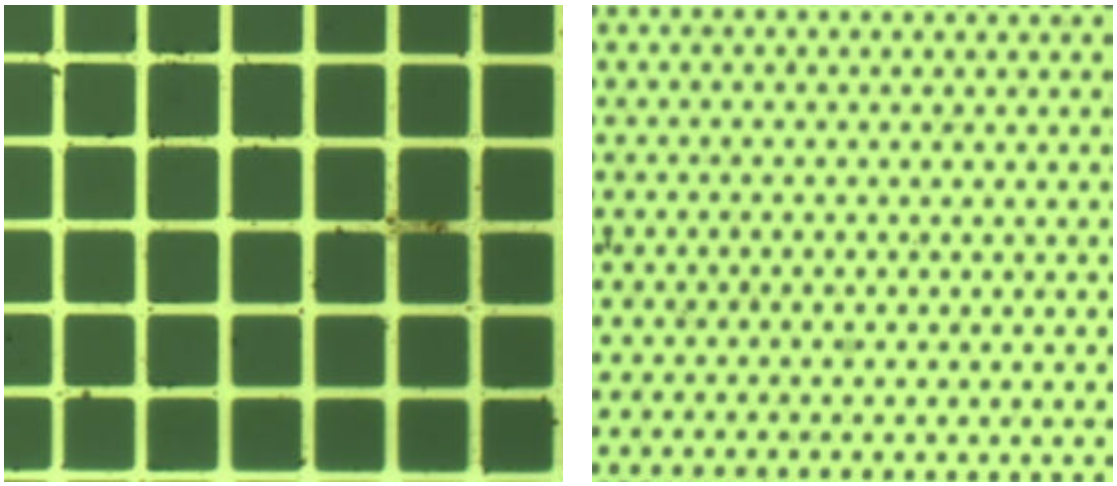

Figure 26. Optical microscope images of the glass-chromium masks used for microcontact printing experiments. On the left: 10 μm wide squares, separated by 2 μm lines. On the right: 2 μm circles separated by 2 μm. When a positive resist is used, these masks create holes of subsequently 10 μm and 2 μm onto the resist.

After the exposure, a development of the resist was done with the developer, *(AZ351B developer Clariant, Germany*) a sodium hydroxide (NaOH) based solution for 60 seconds, removing the exposed areas that became soluble in the developer, thus creating the desired hole pattern. After development, a post exposure bake in 120ºC for 20 minutes was done to strengthen the resist and improve its adhesion.

4.1.1.3 Reactive Ion Etching of Nitride

Using the patterned resist as an etch mask, the nitride was etched using a reactive ion etching (RIE) system (*Oxford 80+, Oxford Instruments Plasma Technology, UK*). The etch gases were trifluoromethane (CHF_3) and oxygen (O_2). Etching time was typically $9-10$ minutes. The parameters for etching are presented in Table 5. To ensure complete etching through the whole nitride film, a slight overtime was used. Slight over etching is not harmful, but if some of the nitride would be left, the following wet etching of silicon would not start. After the etching step, the remaining resist was removed in an acetone bath with ultra-sound for 10 minutes and then rinsed with acetone and isopropanol (IPA) for 5 minutes each.

Table 5. The parameters for etching nitride with RIE.

CHF_3	50 sccm
O_2	5 sccm
RF-power	150 W
Pressure	55 mtorr

4.1.1.4 Tetramethyl Ammonium Hydride Etching of Silicon

The inverted pyramid shape was achieved with anisotropic etching of silicon. In some etchants, the etch rate is different for different crystal planes of silicon, (100) planes are fast etching and (111) planes are slow etching. In (100) oriented wafers the (111) planes produce a sidewall angle of 54.7°, as depicted in Figure 27 [2].

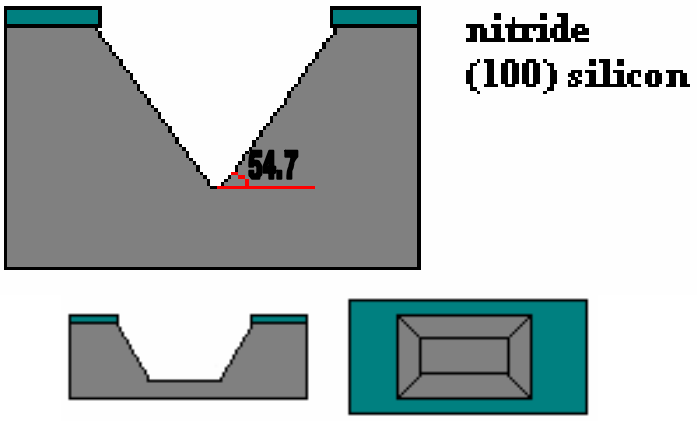

Figure 27. Anisotropic etching of (100) silicon. The (111) planes etch slower, forming a sidewall angle of 54.7°. A cross section model of a (100) silicon etched anisotropically, and a top view. The (111) sidewalls etch slower, forming a 54.7° angle and eventually come together forming an inverted pyramid shape when a square mask opening is used.

The wafers were anisotropically etched with a 25 % solution of tetramethyl ammonium hydroxide (TMAH, $(CH_3)_4NOH$) in deionized water (DI-water). The patterned nitride film was used as an etch mask. The etching was done in a quartz vessel bath that was heated; the

etching temperature was 83°C. The etch rate in TMAH at 80°C is approximately 0.45 – 0.7 µm/min. The n and p type silicon might have slightly different etch rates in TMAH, as well as differently doped wafers; highly doped silicon has a slower etch rate. Slight over etching is not harmful, since the goal is to produce a very sharp tip for the pyramid. Too long etching, however would eventually connect the holes together, so care must be taken when calculating the time for etching. The depth of an inverted pyramid that is 10 µm wide is approximately 5.5 µm and with a 2 µm wide inverted pyramid, the width is approximately 1.1 µm. Different etching times were tested, and a suitable etching time for n type wafers was found to be 2 – 8 minutes for 2 µm holes, and 10 – 20 minutes for 10 µm holes. After wet etching, the surface of silicon is smooth. A cross sectional and a top view of the inverted pyramids is shown in Figure 28.

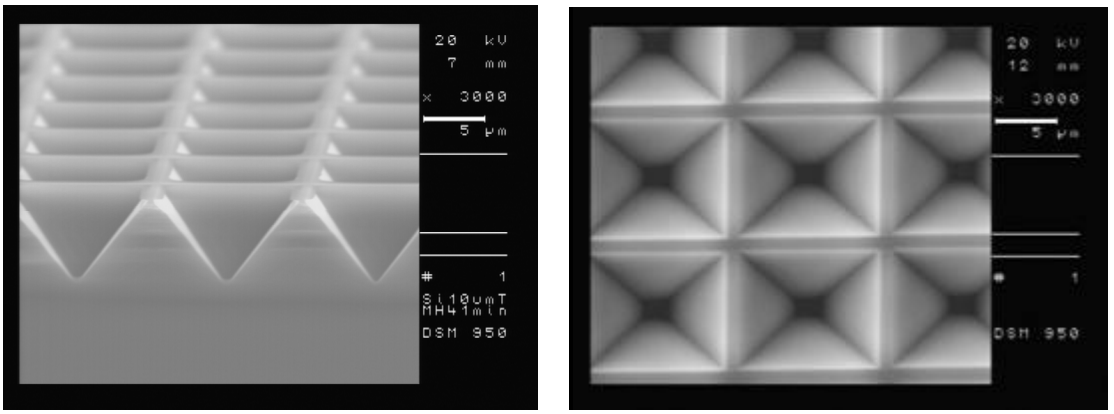

Figure 28. A cross sectional and top view of the inverted pyramids created by anisotropic etching of silicon.

4.1.1.5 Buffered Hydrofluoric Acid Etching of Nitride

Finally, the remaining nitride layer is removed by etching in buffered hydrofluoric acid (BHF) "SiO etch" solution consisting of hydrofluoric acid (HF) and ammonium fluoride (NH_4F) at 32°C. The etch rate for nitrogen in BHF depends greatly on the film quality, concentration and temperature. PECVD nitride etches faster than low pressure chemical vapour deposition (LPCVD) nitride. Etching times used were 20 – 25 minutes, and this was

enough to remove the entire nitride layer. It is important to remove the nitride, since the structure produced by under etching of the nitride layer with TMAH would otherwise prevent the stamp release in the following steps, as shown in Figure 29. After the nitride etching the master is ready to be used for molding.

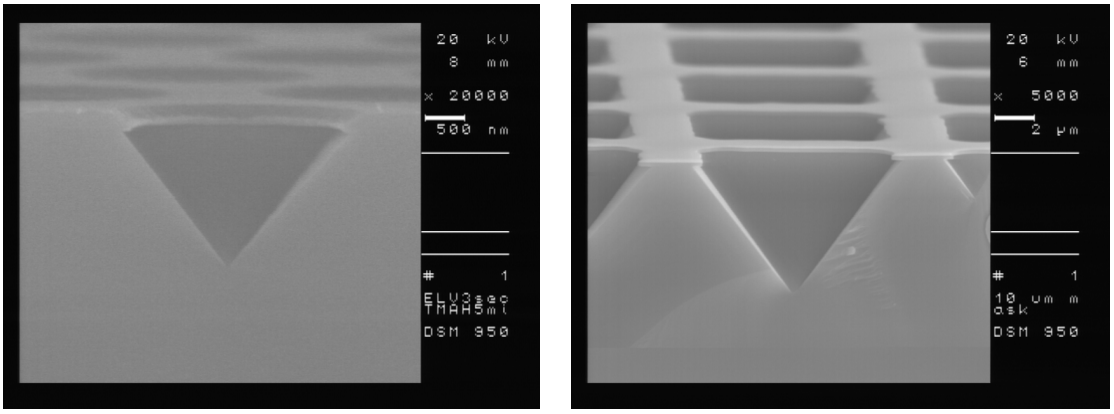

Figure 29. The cross section of the inverted pyramids after TMAH etch, showing the nitride layer on top, that needs to be removed before molding. On the left, a 2 µm circle shaped hole in the mask, the under cutting is produced with the anisotropic etching. On the right a 10 µm wide pyramids.

4.1.2 Photoresist Master

Another design for master is a simple photoresist structure. In this design, the idea is to create low aspect ratio holes in photoresist with the 10 µm and 2 µm holes mask. Standard RCA-cleaned silicon wafers (*Okmetic Ltd, Finland*) were used. The standard photolithography as described in chapter 4.1.1.2 was done, with the *AZ5214E* photoresist and a 4 seconds exposure time. After the hard bake, the masters were ready to use. A positive photoresist profile has a positive slope of 75 – 85° [43], so this shape makes the release of the stamp easy in the molding step.

The exposure time in photolithography affects the size of the exposed areas. If there is a limited amount of radiation, the exposed area is actually smaller than the hole in a mask pattern, and this results in smaller holes when a positive photoresist is used. To test this effect of limiting the amount of exposing radiation, using the 2 µm holes mask, instead of the standard exposure time of 4 seconds, times ranging from 2 seconds down to 0.1

seconds were tested. The photolithography was done as described above in chapter 4.1.1.2, but a thinner positive photoresist (*AZ1505, Clariant, Germany*) was used, creating a 500 nm layer with 4000 rpm and 25 seconds spinning. After the development of the resist and a hard bake, the master was used as such. The fabrication steps of the photoresist master are presented in Figure 30.

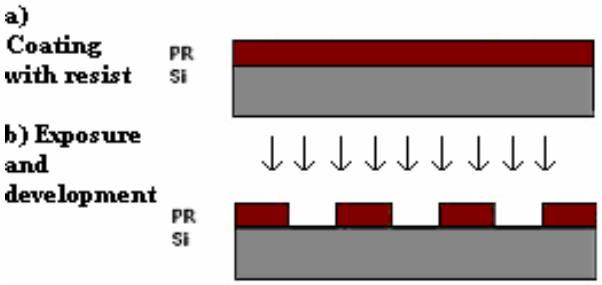

Figure 30. The photoresist master fabrication.

With short exposure times, it is possible that some of the photoresist is not exposed at the bottom of the photoresist layer, thus creating a layer of photoresist remaining on the wafer at the areas of holes as well, as presented in Figure 31. This does not prevent the structure to be used as a master; it only lowers the aspect ratio of the molded PDMS stamp. The aspect ratio of a stamp made with a 2 μm holes mask and 500 nm layer of resist is, depending on the width of the hole, approximately 1:4. These low aspect ratio structures should not have the problem of pairing. The photoresist masters are shown in Figure 32.

Figure 31. The short exposure times may result in a remaining layer of resist also in the areas of holes.

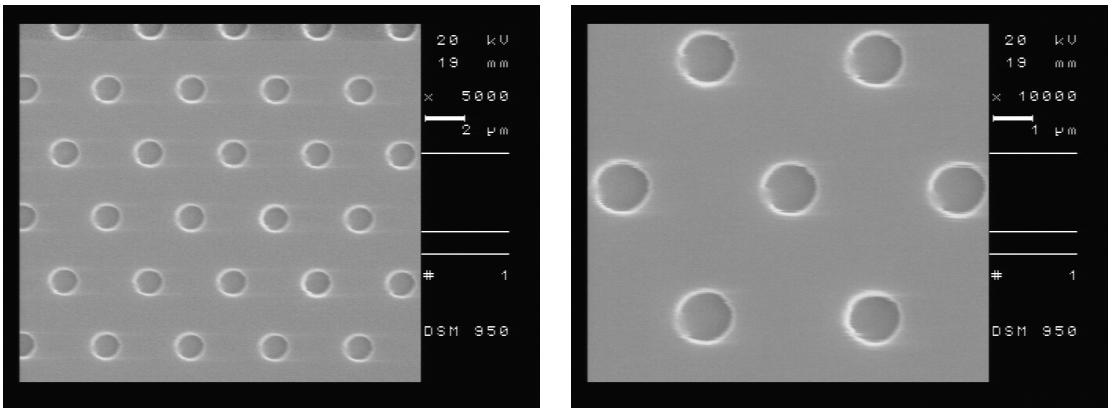

Figure 32. Scanning electron micrographs of a photoresist master created with a 2 seconds exposure time and 500 nm photoresist layer.

4.1.3 DRIE Silicon Master

Another master design is to use cryogenic deep reactive ion etching (DRIE). With the DRIE process it is possible to produce high aspect ratio structures. A standard photolithography was performed on silicon wafers, as described in Chapter 4.1.1.2. After development and hard bake, using the patterned resist as an etch mask, a DRIE etching was done to etch the holes in the silicon wafer. The etching was done using cryogenic DRIE equipment, which has an inductively coupled plasma (ICP) and a capasitively coupled plasma (CCP) power sources. (*Oxford Instruments Plasmalab System100 - ICP 180, UK*). The gases used were sulphur hexafluoride (SF_6) and oxygen (O_2). The parameters of the etch recipe are shown in Table 6.

Table 6. Process parameters in DRIE etching.

SF_6	40 sccm
O_2	6 sccm
ICP power	1000 W
CCP power	3 W
Temperature	–110°C
Process pressure	10 mtorr
Helium backside pressure	5 torr

Etching times of 5 and 2.5 minutes were used, producing masters with holes that have depths of around 7 µm and 3 µm respectively. The width of the holes was approximately 2 µm so that the aspect ratio was 7:2 and 3:2. This is a high aspect ratio compared with the photoresist master design described earlier. After acetone resist removal, the DRIE etched masters needed to be coated with a release layer, otherwise the release of the PDMS stamp failed. The fabrication steps are presented in Figure 33. A cross sectional view of the DRIE master before resist removal is shown in Figure 34.

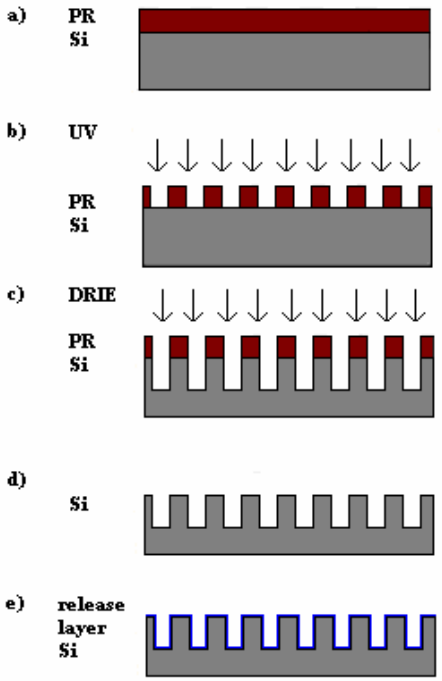

Figure 33. DRIE master fabrication steps.

The release layer coating was done at University of Helsinki, Accelerator laboratory using a method developed by Kiuru et al. [44]. The coating is called diamond-like carbon (DLC), which is a carbon material with sp^3 diamond bonds and is described in reference [44]. The thickness of the coating is 20 – 40 nm.

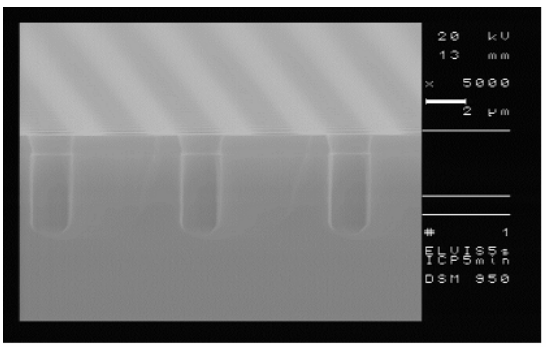

Figure 34. DRIE etched master with the resist still in place.

4.2 Stamp Fabrication

Poly(dimethylsiloxane) (PDMS, 184-PDMS) (*Sylgard ® 184, Dow Corning*) in a commercial kit consisting of a base and a curing agent was used for PDMS stamp fabrication. The two parts were mixed in 10:1 weight to weight ratio, thoroughly stirred and degassed in vacuum for 30 minutes to ensure the removal of the air bubbles created during stirring. After degassing, the prepolymer mixture was poured onto the master and degassed for 5 minutes in vacuum to remove the air bubbles created during pouring. The stamp was cured thermally in temperatures ranging from room temperature to 65°C for up to 48 hours. Typical curing times recommended by the manufacturer are for example 24 hours at room temperature or 4 hours at 65°C. The full mechanical properties appear only after 7 days of curing at room temperature [28]. The process steps in stamp fabrication are presented in Table 7. In its initial state, PDMS is a flowable liquid. When cured, PDMS turns into an elastomeric rubber, and it can be easily removed from the master, using a scalpel to cut it. The thickness of the stamp was typically 2 – 3 mm. Thinner stamps were difficult to release from the master and had a tendency to tear when releasing them from the master. The stamps were cut with the scalpel in pieces of typically 1 – 3 cm^2. A cross sectional view of the molded PMDS in an inverted pyramid master is shown in Figure 35, and top view of the low aspect ratio stamp and pyramid stamp are shown in Figure 36.

Table 7. Fabrication of 184-PDMS stamp.

1.) 20 g of base + 2 g of curing agent
2.) Degassing in vacuum for 30 min
3.) Pouring the mixture onto a master
4.) Degassing in vacuum for 5 min
5.) Curing at 65°C for 24 h

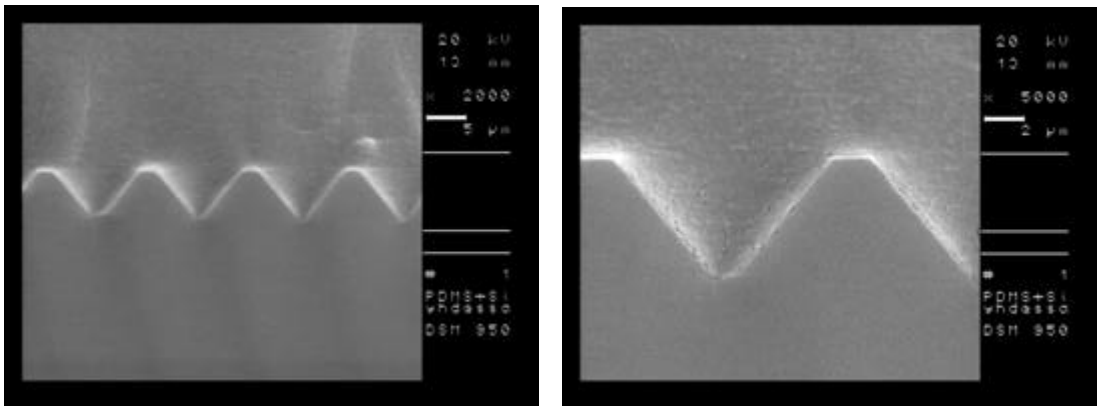

Figure 35. A cross section of 184-PDMS layer inside the master, upper part PDMS, below it silicon pyramid master.

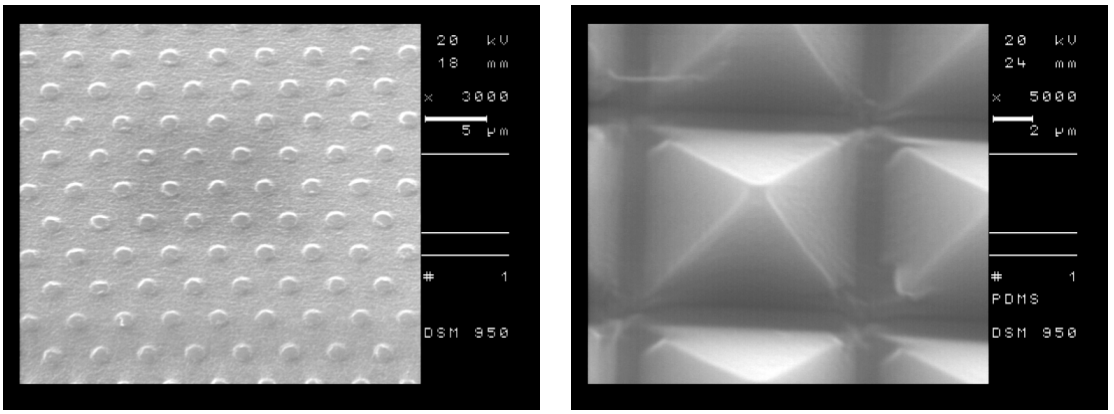

Figure 36. Scanning electron micrographs of the 184-PDMS stamps. On the left, a stamp fabricated by the photoresist master with a 2 µm holes mask, having approximately 2 µm protruding dots, and on the right side, a stamp fabricated with the pyramid master, having pyramids of diameter 10 µm.

4.2.1 Composite Stamp Fabrication

Another material that was used for stamp fabrication was h-PDMS. Composite stamps made of a sandwich structure with 184-PDMS and h-PDMS were tested according to a recipe developed by Schmid et al. [35] and a composite stamp structure modified by Odom et al. [34].

To prepare h-PDMS, first 3.4 g of vinyl PDMS prepolymer (*VDT-731, ABCR GmbH, Germany*), 17.5 µl of platinum-divinyltetramethyldisiloxane, (*ABCR GmbH, Germany*) and 5 µl of 2,4,6,8–tetramethyl-2,4,6,8-tetravinylcyclotetrasiloxane (*ABCR GmbH, Germany*) were mixed and degassed in vacuum for 2 minutes. Then, 1 g of hydrosilane prepolymer

(*HMS-301, ABCR GmbH, Germany*) was added to the mixture. Then the liquid prepolymer mixture was poured onto the master and spun on a self-made spin-coater for 1 – 2 minutes. After spinning, the mixture was cured at 60ºC for 30 minutes and the 184-PDMS prepolymer mixture, prepared as described earlier, a 10:1 weight to weight ratio of base and curing agent, was added on top of h-PDMS mixture. Then the bilayer structure was cured at 60ºC for 24 hours. The fabrication of a composite stamp is presented in Figure 37 and the recipe for the composite stamp fabrication is presented in Table 8.

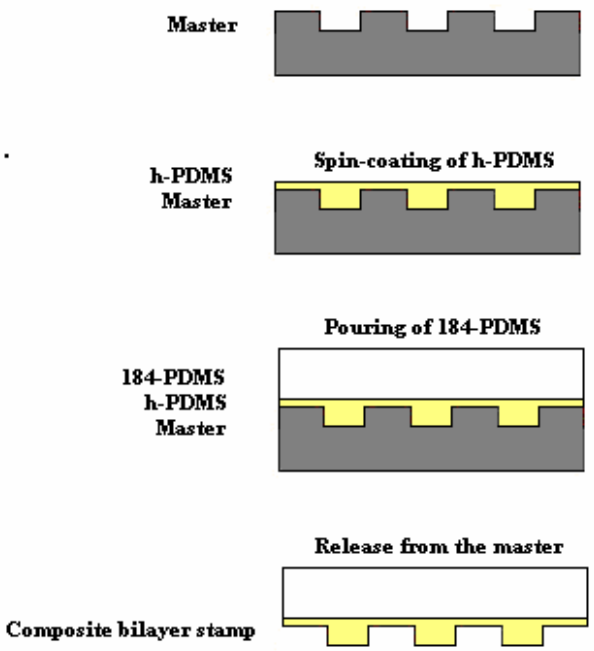

Figure 37. Preparation of the composite stamp of h-PDMS and 184-PDMS.

The release of a composite stamp was more difficult than the release of 184-PDMS stamp. The composite stamps had a tendency to tear and crack, due to their more brittle structure [35]. The area of the stamp that could be used was small compared with the 184-PDMS stamps where the entire stamp is of good quality. The parts of the stamp that did not crack were used for further experiments in this work.

Table 8. Fabrication of the bilayer stamp.

1.) 3.4 g of VDT-731

2.) 17.5 µl of platinum divinyltetramethyldisiloxane

3.) 5 µl of 2,4,6,8-tetravinylcyclotetrasiloxane

4.) Mixing, stirring lightly

5.) Degassing in vacuum for 2 min

6.) Adding of 1 g of HMS-301

7.) Pouring the mixture onto the master

8.) Spinning for 1 – 2 min

9.) Curing at 65°C for 60 min

10.) Preparing of 184-PDMS (10:1 w:w ratio, described in 4.2)

11.) Pouring of 184-PDMS layer on top of h-PDMS layer

12.) Curing the bilayer structure in 60°C for 24 h

4.3 Gold Coating of the Substrate

In this chapter, the physical vapour deposition methods for gold coating are presented, followed by description of the process used in this work.

4.3.1 Physical Vapour Deposition of Gold

Physical vapor deposition (PVD) of thin metal films includes sputtering and evaporation. In PVD methods the material to be deposited is ejected from a solid target in vacuum and transferred onto the substrate surface.

4.3.1.1 Sputtering

In sputtering, energetic ions, usually of argon (Ar^+), hit the surface of a target material, which is in negative potential. Target atoms are ejected, vaporized and transported onto the substrate surface.

Sputtering pressures are usually in the range of 10^{-1}–10^{-4} torr [45], and due to relatively low vacuum, sputtered atoms collide before reaching the substrate, resulting in the coating of also the vertical surfaces [2]. The ideal case is depicted in Figure 38 on the right side.

4.3.1.2 Evaporation

In evaporation, the metal to be deposited is heated in a crucible until it evaporates. The evaporated atoms are transported onto the substrate and condensed. The heating of the material can be done with electron beam (e-beam), when a high current beam scans and heats the material. The heating can also be achieved by direct resistive heating; this method is called thermal evaporation.

The pressure in evaporation is usually 10^{-6} – 10^{-9} torr [45]. In high vacuum, the atoms do not collide with each other, and therefore they cover only the surfaces parallel to the beam, as presented on the left side in Figure 38.

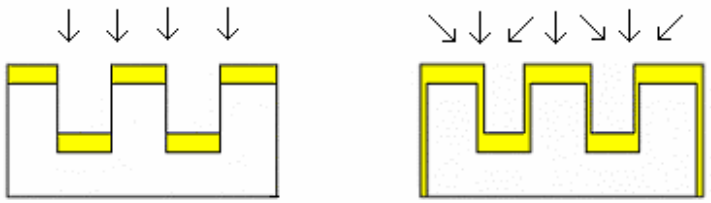

Figure 38. Step coverage in evaporation (left) and sputtering (right). This is an ideal case; in reality the coverage is more uneven.

A thin film of gold was deposited onto silicon substrates. To enhance the adhesion of gold, an adhesion layer of tungsten (W), chromium (Cr) or titanium (Ti) was deposited under the layer of gold. Two different evaporation methods to deposit the gold were used: a thermal evaporator (*Edwards, 304 UK*) and an in-house-built electron beam (e-beam) evaporator.

Prior to the evaporation with the thermal evaporator, an adhesion layer was deposited onto the silicon wafers. A sputter (*Oxford, UK*) was used for the deposition of 10 – 20 nm of

chromium or tungsten. On top of the adhesion layer, approximately 100 nm layer of gold was thermally evaporated.

In the electron beam evaporator, it was possible to deposit the adhesion layer in the same vacuum as the gold layer. The adhesion layers deposited were of titanium, thicknesses of 1 – 10 nm and the gold layers of 20 – 100 nm. Both methods of evaporation and all the different adhesion layers and layer thicknesses resulted in fairly good adhesion of the gold and the different films proved to be suitable for microcontact printing. After the coating, the substrates were cut to pieces of 3 – 4 cm^2.

4.4 Printing Procedure

4.4.1 Eicosanethiol Solution Preparation

Eicosanethiol (ECT) (*Robinson Brothers Ltd, UK*) solution was prepared diluting ECT grains in 96.1 vol% ethanol (*Altia, Finland*). ECT concentration of solution was 0.2 mM. To facilitate the dilution of ECT, the solution was placed on a stirrer for 5–6 hours. After this time the grains were thoroughly dissolved in ethanol. Without stirring, the grains still were insoluble after 24 hours. The solutions were stored in sealed containers protected from light, and fresh solutions were fabricated weekly, to ensure the freshness of the solution.

4.4.2 Inking of the Stamp

The stamps were inked using two different methods; wet inking and contact inking as presented by Libioulle et al. [46].

4.4.2.1 Wet Inking

Wet inking is a method in which a drop of solution is placed onto the stamp, then the stamp is dried and a layer of ink will be left on the stamp, as shown in Figure 39. The wet inking method is the simplest inking method, but it has the problem with diffusion as discussed in chapter 3.2.2 and in Figure 24 [46].

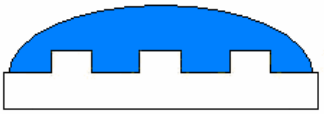

Figure 39. Wet Inking.

The stamps were coated with a droplet of solution for 2 minutes. The excess ink was dried with a nitrogen flow for 30 – 40 seconds. The stamp was immediately placed onto the substrate, with its own weight.

4.4.2.2 Contact Inking

Contact inking is a method used for limiting the diffusion of the ink solution [46]. This method uses an ink pad, which is immersed in the ECT solution, and the stamp is inked with this pad, as shown in Figure 40.

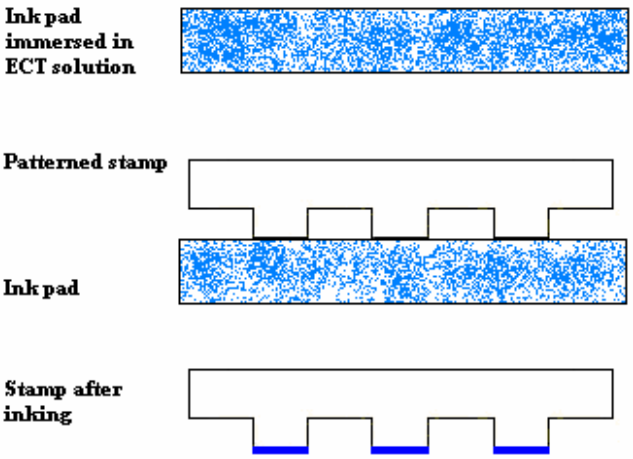

Figure 40. The principle of contact inking.

An unpatterned bulk piece of PDMS is used as the ink pad. The PDMS was prepared as described above, but cured in a petri dish without a master, and cut into pieces of approximately 3 – 4 cm^2. The thickness of the ink pad was around 2 mm. The ink pad was immersed in the ECT solution for at least 24 hours. It was dried with a stream of nitrogen for 30 – 40 seconds, and a patterned stamp was placed on top of it with the patterns faced down, with its own weight allowing ideally only the protruding features of the stamp to be coated in the solution. The inking times used were typically from 40 – 60 seconds. After the inking, the stamp was immediately used for printing.

4.4.3 Printing

After inking, the stamp was placed onto the gold-coated substrate. The printing times used were from 30 seconds to 3 minutes. No excess weight was applied onto the stamp. The ECT was transferred from the stamp onto the gold film and SAM was formed on the areas of the contact between the stamp and substrate as presented in Figure 41. The diffusion of the thiol widens the pattern from the original area of contact.

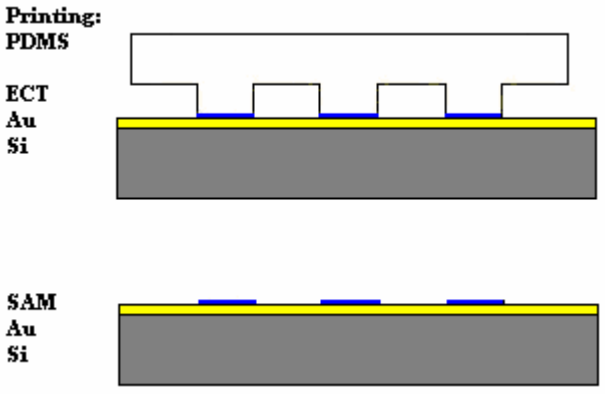

Figure 41. Transfer of ECT, this is an ideal case. In reality there is some diffusion of the pattern.

4.5 Etching

The etching using the printed SAM as an etch mask was done with ferric(III)nitrate nonahydrate ($Fe(NO_3)_3 \cdot 9H_2O$) (*Tamro, Finland*), powdery grains and thiourea (CH_4N_2S) (*Tamro, Finland*), a fine powder. The solution consisted of 20 mM ferric(III)nitrate and 30 mM thiourea in deionized water (DI-water) according to a recipe of Geissler et al. [18]. The pH of the etchant is controlled with hydrochloric acid (HCl), and in this work it was in the range of 0 – 2. The printed substrates were placed into the etching solution, keeping them under the liquid and occasionally stirring very lightly. The etching was performed at room temperature. The etching times used were 8 – 12 minutes. After etching, the substrates were rinsed in DI-water.

4.6 Transfer of Gold onto Silicon

It was also tested whether it is possible to use gold as the "ink" material and transfer it onto a silicon substrate that was immersed in eicosanethiol solution. In this version of transfer printing the ECT solution used to pre-treat the substrate does not form a self assembled monolayer onto its surface. The solution was changing the surface of silicon, but it is not possible to form a self assembling monolayer on silicon or silicon dioxide with eicosanethiol. The idea in this experiment was to test whether the gold could still have a stronger adhesion onto the pre-treated substrate than to the stamp, and thus enable the transfer. The procedure used in this work is presented in Figure 42. The fabrication steps are presented in detail in the following chapters, starting with the master fabrication in Chapter 4.7. The stamp fabrication procedure is the same as in the case of microcontact printing, as described earlier in Chapter 4.2. The gold coating of the substrate is presented in Chapter 4.9 and the procedure of substrate pre-treatment in Chapter 4.8 and printing in Chapter 4.10.

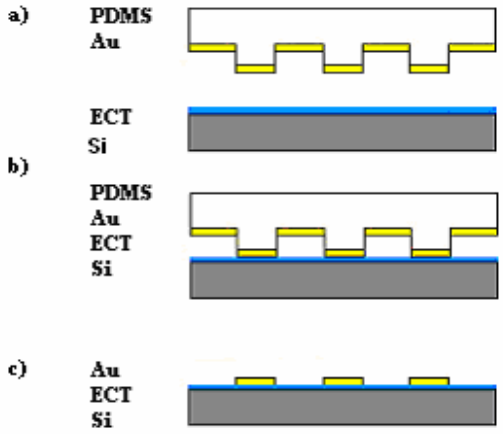

Figure 42. Transfer printing: a) evaporation of gold, immersion of the substrate in ECT b) printing c) transfer of gold pattern.

4.7 Master Fabrication for Transfer Printing

For the transfer printing experiments, the master has to have vertical sidewalls, because the PDMS molded of it will be coated with evaporated gold. The technique succeeds only if the gold is deposited on the horizontal levels of the stamp, thus the sidewalls must not be covered with gold. For this reason, the pyramid master is not applicable. Instead, the simple photoresist design was used, as described in Chapter 4.1.2. The idea was to produce the stamps with short pillars with the 10 µm and 2 µm masks shown in Figure 26. The short exposure times with 2 µm masks were also tested in order to create smaller pillars. The masters are fabricated the same way as the photoresist masters for microcontact printing, described in Chapter 4.1.2 and presented in Figure 30 and Figure 31.

4.8 Substrates for Transfer Printing

Silicon wafers were used as a substrate for these experiments. To make their surface smoother and to ensure uniform wetting, they were oxidised in plasma chamber. A plasma oxidizing chamber TePla 400 (*Techni Plastics, Germany*) was used, the power of 400 W, oxidizing time 10 seconds with 1800 sccm oxygen. Immediately after oxidation the wafers were cut in pieces of approximately 3 – 4 cm^2 and immersed in ECT solution, prepared as

described in Chapter 4.4.1. The immersion times were typically 24 hours. After the immersion time, the substrates were removed from the solution and dried under a stream of nitrogen typically for 30 – 60 seconds. The silicon substrate with or without an oxide layer is not a suitable substrate to form a self assembling monolayer with eicosanethiol, and gold is not adhered onto an untreated silicon substrate. The surface is modified by the immersion in ECT in a way, that gold can adhere to it.

4.9 Gold Coating of the Stamp

A layer of gold was deposited onto the stamps, only at the horizontal surfaces. The deposition was made by evaporation, since sputtering would cover also the sidewalls. The adhesion layer was not used in this case because the idea is to have a poor adhesion between gold and PDMS, so that the adhesion between the silicon and gold would be greater than that of PDMS and gold, thus transferring the gold layer from the stamp to the substrate at the regions of contact. The thickness of the gold layer is approximately 20 nm.

4.10 Printing

The gold-coated stamp was placed onto the substrate and pressed hard for 30 – 60 seconds. Then it was removed gently. The gold pattern was formed from the protruding features of the stamp onto the silicon substrate.

4.11 Contact Angle

The angle q, between the solid surface and the tangent to the liquid surface at the line of contact with the solid, is known as the contact angle, as shown in Figure 43. When the liquid used is water, a surface that has polar groups, for example hydroxyl groups, has a

good affinity for water, thus strong adhesive forces and a low contact angle. Such a surface is hydrophilic and the contact angle is smaller than 90°. If the surface has non-polar groups, for example polymer surfaces or organic layers, the contact angle is large, over 90°, and the surface is hydrophobic. Measurement of contact angle is a simple method to get qualitative information of surfaces.

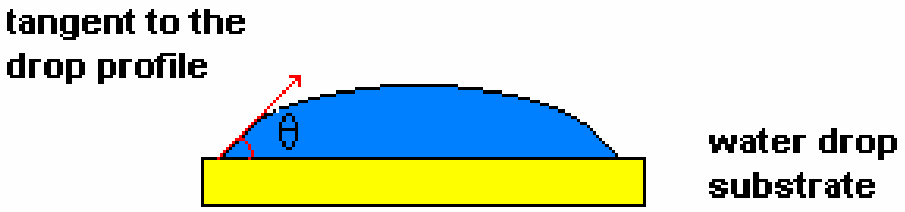

Figure 43. Definition of contact angle.

5 Results

The stamps and substrates were inspected with an optical microscope and with a scanning electron microscope (*Opton*) operating at 20 kV. The low aspect ratio stamps were fabricated of the regular 184-PDMS, and for the pyramid stamps both 184-PDMS and composite bilayer stamps were tested.

For the purpose of easier following of the results, the low aspect ratio stamps fabricated with the limited exposure time masters are named after the exposure times, and presented in Table 9.

Table 9. The nomenclature for low aspect ratio stamps used in this work.

Nominal size of the master pattern defined by the photomask	Exposure time in master fabrication	Name for the stamp
10 μm diameter holes	4 seconds	10μm-stamp
2 μm diameter holes	2 seconds	2sec-stamp
2 μm diameter holes	1.5 seconds	1.5sec-stamp
2 μm diameter holes	1 second	1sec-stamp
2 μm diameter holes	0.5 seconds	0.5sec-stamp
2 μm diameter holes	0.4 seconds	0.4sec-stamp
2 μm diameter holes	0.3 seconds	0.3sec-stamp

5.1 Inspection of the Low Aspect Ratio Stamps

A scanning electron micrograph of a low aspect ratio 10μm-stamp is shown in Figure 44. 2sec-stamp, 0.4sec-stamp and 0.3sec-stamp are presented in Figure 45. The protruding features can be clearly seen even in the low aspect ratio structures

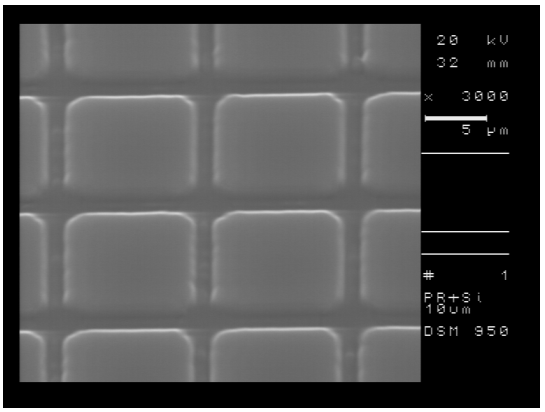

Figure 44. PDMS 10㎜m-stamp having 10㎜m wide protruding features separated by 2 ㎜m wide valley areas.

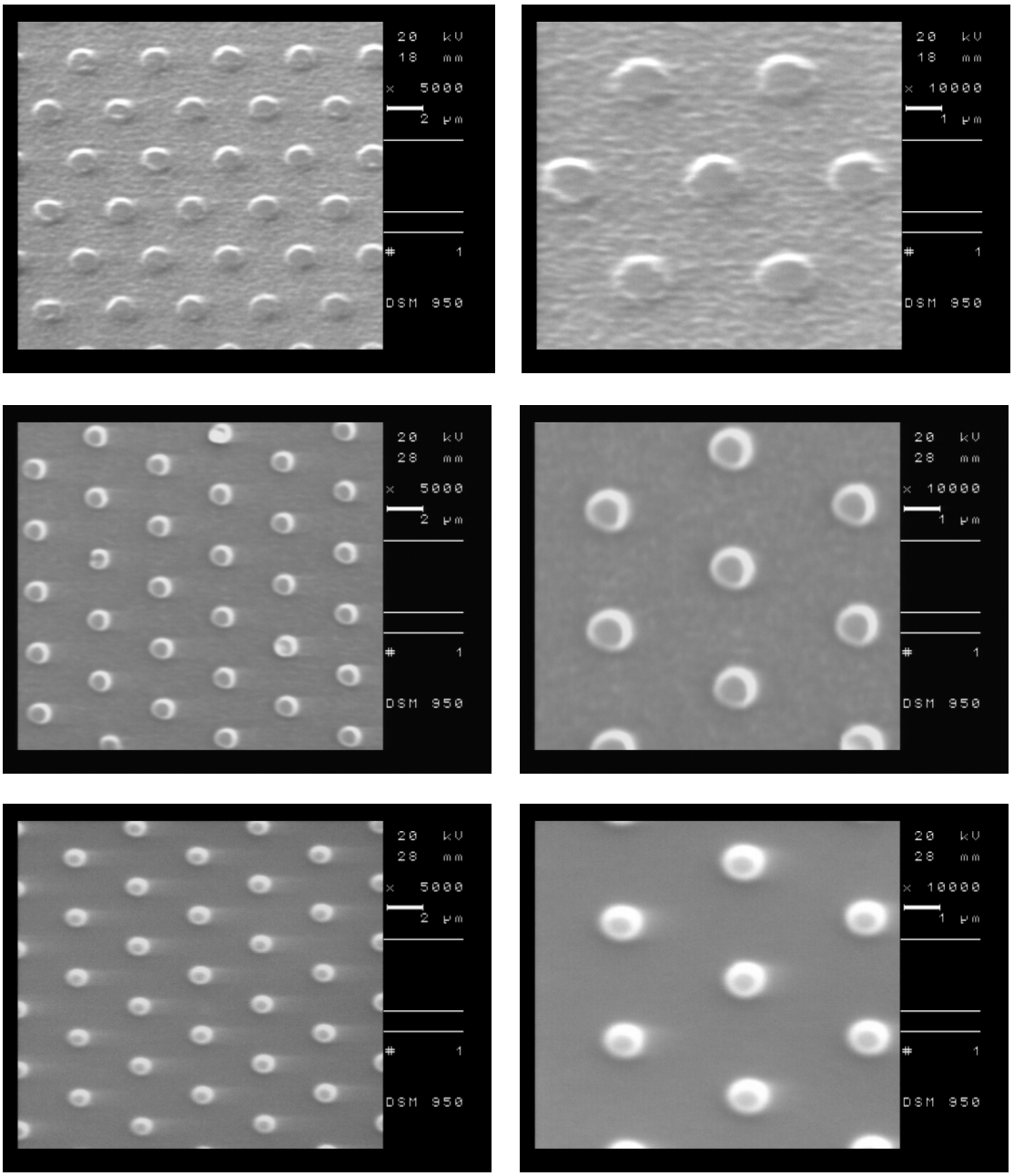

Figure 45. The low aspect ratio PDMS stamps. Top row: 2sec-stamp, second row: 0.4sec-stamp, third row: 0.3sec-stamp.

The photoresist masters with the exposure times down to 0.3 seconds produced deep enough holes that they could be used as master. Exposure times less than 0.3 seconds however failed to produce good masters.

5.2 Inspection of the Pyramid Stamps

The pyramid stamps are shown in Figure 46. In the first row, the stamp is made of 184-PDMS, and in the second row the stamp is a composite bilayer h-PDMS stamp. The tip of the pyramid is around 500 – 1000 nm wide. It can be seen that the edges of the pyramid and the tip are not ideally sharp but a bit rounded. Rounding is due to the surface tension of PDMS as described in chapter 3.1 and references [34, 36], and thus cannot produce a very sharp tip to print small features ideally. With h-PDMS it should be possible to achieve sharper features, but in the scanning electron micrographs in Figure 46 it is difficult to tell whether h-PDMS pyramid has a sharper tip than the 184-PDMS.

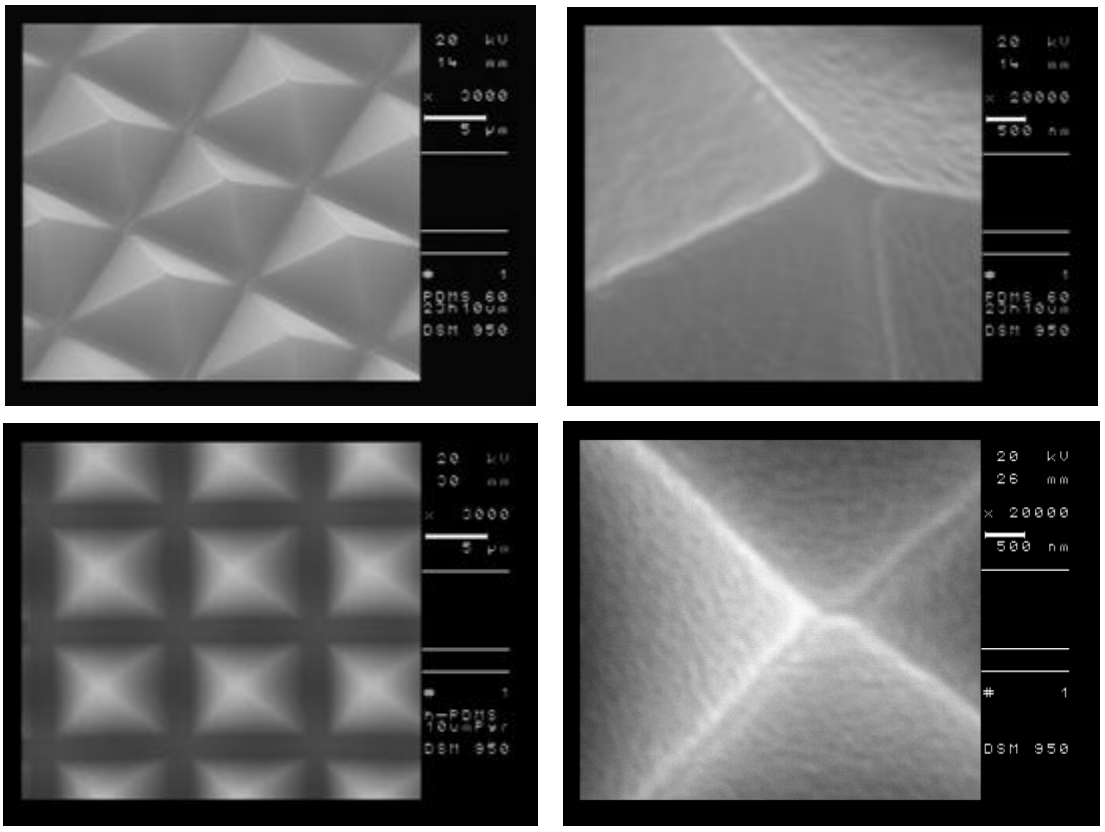

Figure 46. Pyramid stamp. Top row: 184-PDMS, bottom row: h-PDMS. The tip of the pyramid is around 500 nm in both cases.

5.3 Inspection of the High Aspect Ratio Stamps

With the high aspect ratio DRIE master design, a release layer must be used. Without a release layer, the PDMS stamp could not be completely released of the master, but it was torn resulting in the cutting of protruding features, as shown in Figure 47, the image in the top left corner shows a cross section of the master having the protruding features of the stamp that were not released. In the other images, the top view of the stamp is pictured, showing the cutting of the PDMS pillars.

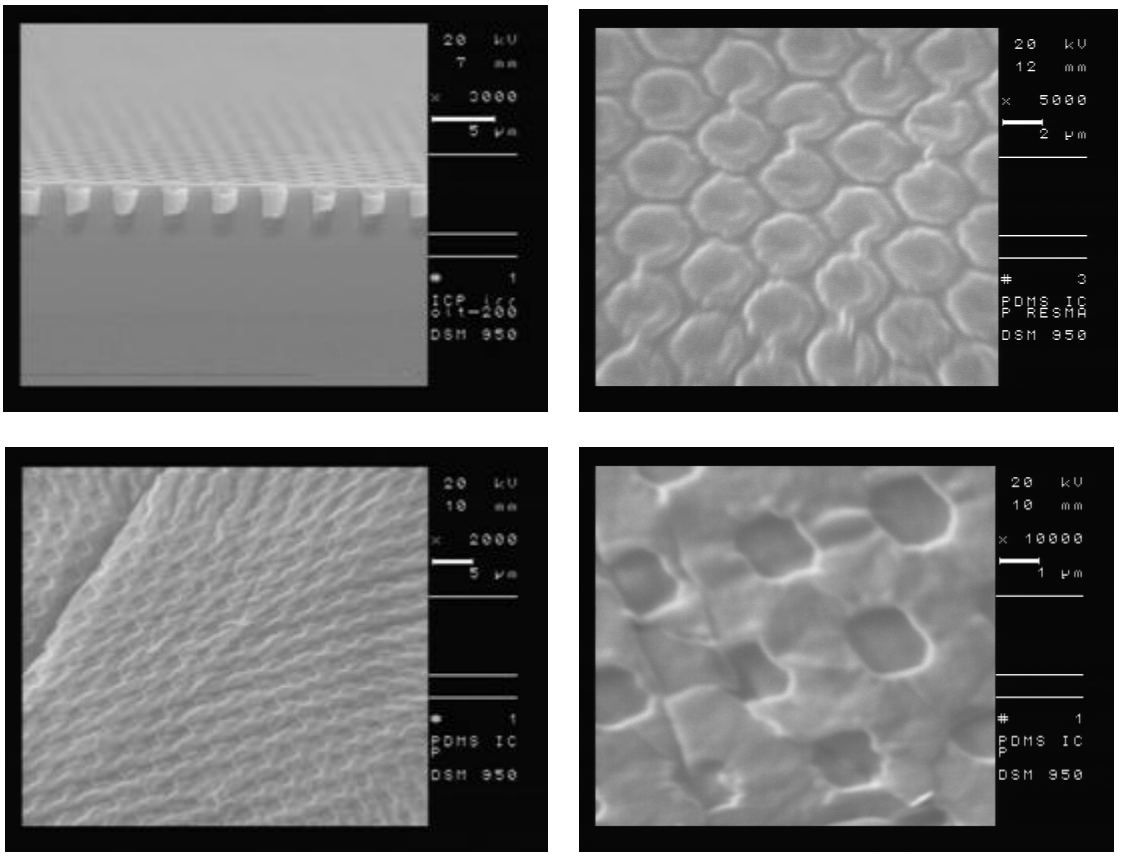

Figure 47. Stamp fabrication with DRIE master without a release layer. On the top left image, a cross section of the master after the release of the stamp, the polymer is not released of the holes, but is torn. Top right image and bottom row images show the stamp after the release, no pillars but holes.

The release of the stamp is successful for a DRIE master when a release layer is used, as shown in Figure 48.

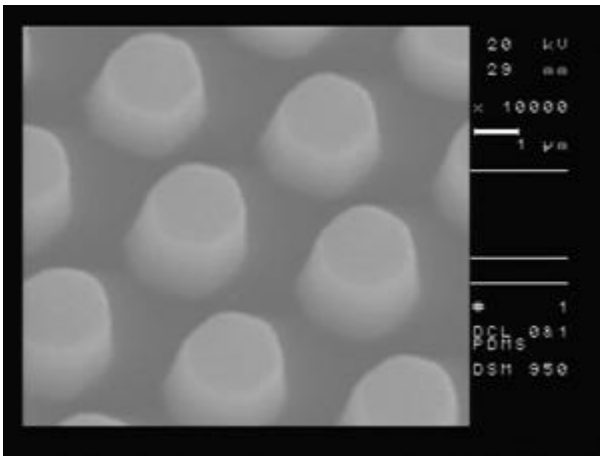

Figure 48. PDMS stamp fabricated with a DRIE master and release layer coating.

A release layer coating allows the release of stamp of the DRIE master. The coating layers used for this work were made at the University of Helsinki, Accelerator Laboratory and the coating materials were based on diamond like carbon (DLC), in Figure 48, the coating used for release was 30 – 40 nm of diamond-like carbon - poly(dimethylsiloxane) -hybrid (DLC-PDMS-h), described in reference [44].

Higher aspect ratio structures, however, have tendency of pairing, due to PDMS properties as described in chapter 3.1. This effect can be seen in Figure 49, the PDMS stamp made of DRIE master and a 20 nm coating of diamond-like-carbon-polytetrafluoroethylene-hybrid (DLC-PTFE-h), described in reference [44].

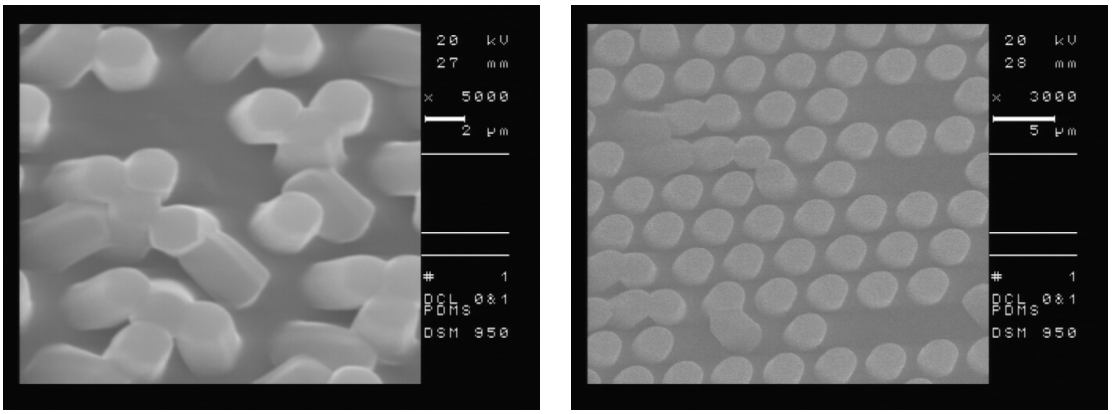

Figure 49. The pairing of features with higher aspect ratio is typical for PDMS.

Based on these results of stamp fabrication, for the microcontact printing experiments the low aspect ratio photoresist masters and inverted pyramid masters were chosen because they seemed most suitable for this application. The higher aspect ratio in DRIE masters causes pairing of the pillars in the stamp, and this is not a problem with the low aspect ratio and pyramid shaped stamps, which do not have a tendency of pairing and neither do they require a release layer coating. For the transfer printing experiments, the low aspect ratio photoresist masters were chosen for their ease of fabrication and the suitable shape. The stamp for this application has to have vertical sidewalls and thus pyramid stamp shape is not suitable.

5.4 Measurements of Water Contact Angle

The time of formation of the SAM was tested using water contact angle (q) measurement. The gold-coated silicon wafer was cut into pieces of approximately 4 cm^2 and placed in a 0.2 mM ECT solution for times varying from 30 seconds up to 15 minutes. After the immersion time, the sample was dried with a stream of nitrogen, and a drop of water was placed onto the surface. A computer software (*Cam 100*) was used to calculate the contact angle. According to these measurements, the surface of the gold layer was initially weakly hydrophilic, having the contact angle of around 87°. After only 30 seconds immersion in ECT solution, the surface had turned hydrophobic, having a contact angle of approximately 110°. The result remained the same after 3, 5 and 15 minutes immersion, so the monolayer formation is assumed to be completed in 30 seconds

The difference between a printed layer of SAM on gold and a layer formed by immersion of the substrate in the solution was also tested by comparing the contact angles in both cases. The printing in this experiment was done with an unpatterned bulk piece of PDMS, ideally resulting in a layer of SAM onto the whole substrate surface area. The unpatterned PDMS stamp was immersed in the 0.2 mM solution of ECT in ethanol for 48 hours. The printing of an untreated gold-coated substrate was done immediately after the removal and

drying with nitrogen of the unpatterned stamp. The printing times tested were from 30 seconds up to 3 minutes

According to these measurements SAM is not formed as perfectly with 30 seconds printing as with 30 seconds immersion. Contact angles were measured in both types of samples, and it showed a difference between them. After 30 seconds, the SAM formed by printing had a q of 90° and the SAM formed by immersion showed a q of 110°. With a 1 minute printing time, the printed SAM showed to be relatively similar to the immersed SAM, the result having no notable difference with longer printing times than 1 minute. There is however a difference between the layers formed in 30 seconds printing and 1 minutes printing, and this is important, since the printing time in microcontact printing has to be limited in order to avoid the diffusion of the printed features. The data of the contact angle measurment results can be seen in Appendix A.

5.5 Microcontact Printing Results

5.5.1 Microcontact Printing with Low Aspect Ratio Stamps

For the nomenclature of the low aspect ratio stamps, refer to Table 9. The first experiments were performed with a 10µm-stamp and wet inking. The printed pattern after etching, silicon squares on gold is shown in Figure 50. The gold is etched at the areas not protected by the SAMs, but the edges of the features are not even, this could be due to diffusion or unevenness of the stamp and conformal contact itself.

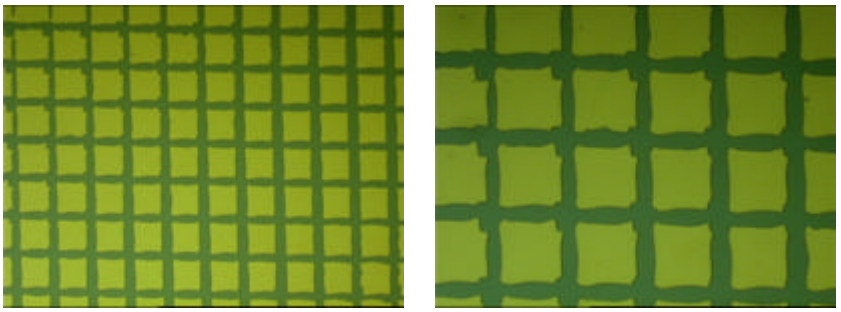

Figure 50. Optical microscope images of gold patterns on silicon created with μCP with 10μm-stamp, wet inking.

Scanning electron micrographs in Figure 51 show the gold dot pattern that was printed using the 2sec-stamp and wet inking. An array pattern of gold dots can be seen.

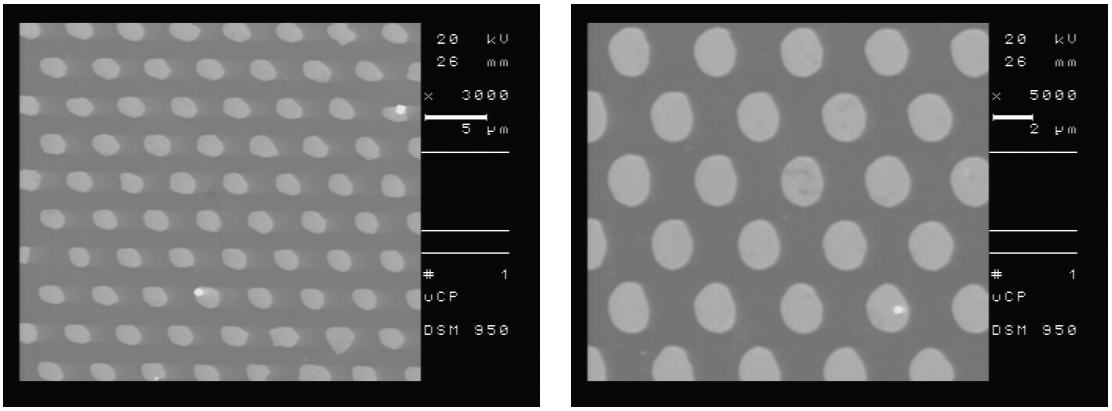

Figure 51. μCP gold dots made by wet inking by 2sec-stamp.

5.5.1.1 Size Variation at the Edges of the Printed Features

The size of the dots has some variation, however. Especially near the edges of the stamp, the dots tend to be smaller, as can be seen in Figure 52. With the same magnification the dots, which are at the edge of the printed pattern (Figure 52, on the left), are of different size, when compared with the dots on the central area of the print (Figure 52, on the right). This might be due to uneven pressure caused by the stamp during printing, or stamp thickness variation at the edges. The cutting of the stamp with a scalpel might also cause distortion of the features at the edges of the stamp. Because of this, the pictures presented in this work are taken at the central area of the printed pattern unless otherwise stated.

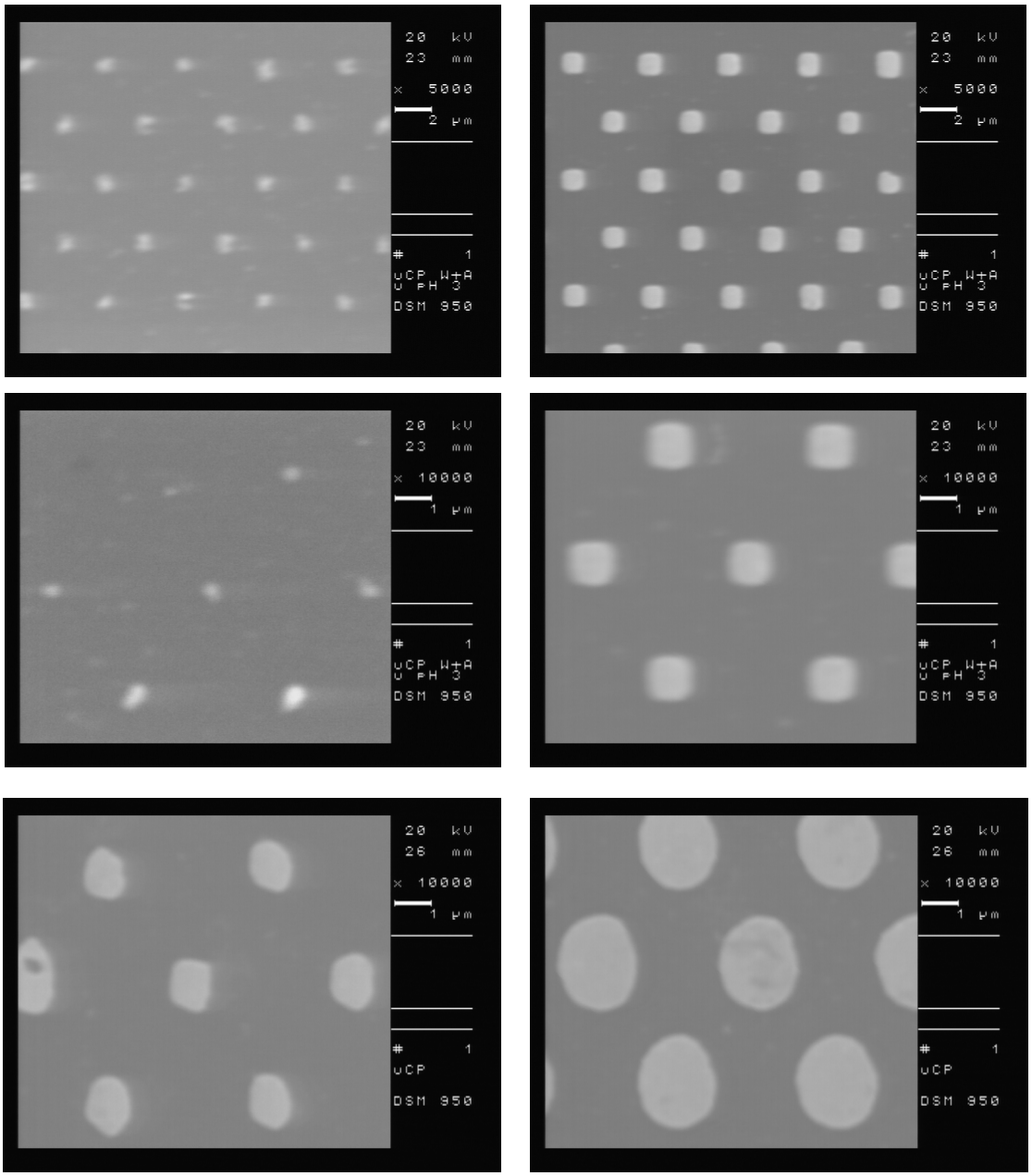

Figure 52. Microcontact printed gold dots on silicon. The size of the dots varies at the edge of the stamp. The left side pictures are taken at the edge of the stamp and the right side pictures are taken at the center of the stamp. First and second row: 0.3sec-stamp, wet inking, third row: 2sec-stamp, wet inking.

5.5.1.2 Periodical Size Variation of the Printed Features

The variation of the size in the patterns made with the 2 µm hole mask, having a periodical pattern of smaller and larger dots is presented in Figure 53. The reason for this is the 2 µm holes photomask that is not of very good quality. The mask was purchased without proper metrology and quality checks because it is just for testing of patterning and not for production where yield would be important. The mask has some variation in the pattern size, and the effect gets stronger when exposure times below the standard 4 seconds are used.

Because of this variation in the pattern size, all the pattern pictures presented in this work are taken of the area at the period where the features are smaller, so the different stamps can be compared as accurately as possible.

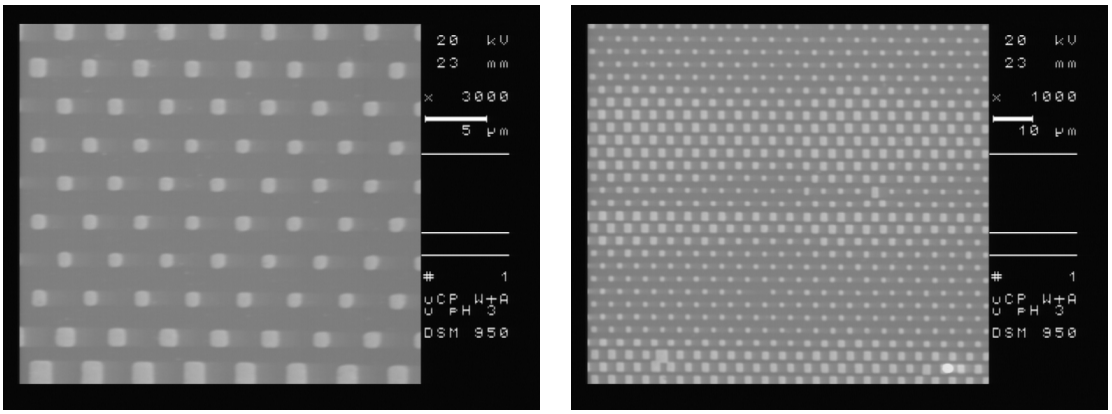

Figure 53. Microcontact printed pattern of gold dots on silicon. The variation of pattern size can be seen in these images. This printing was made with a 0.3sec-stamp, wet inking.

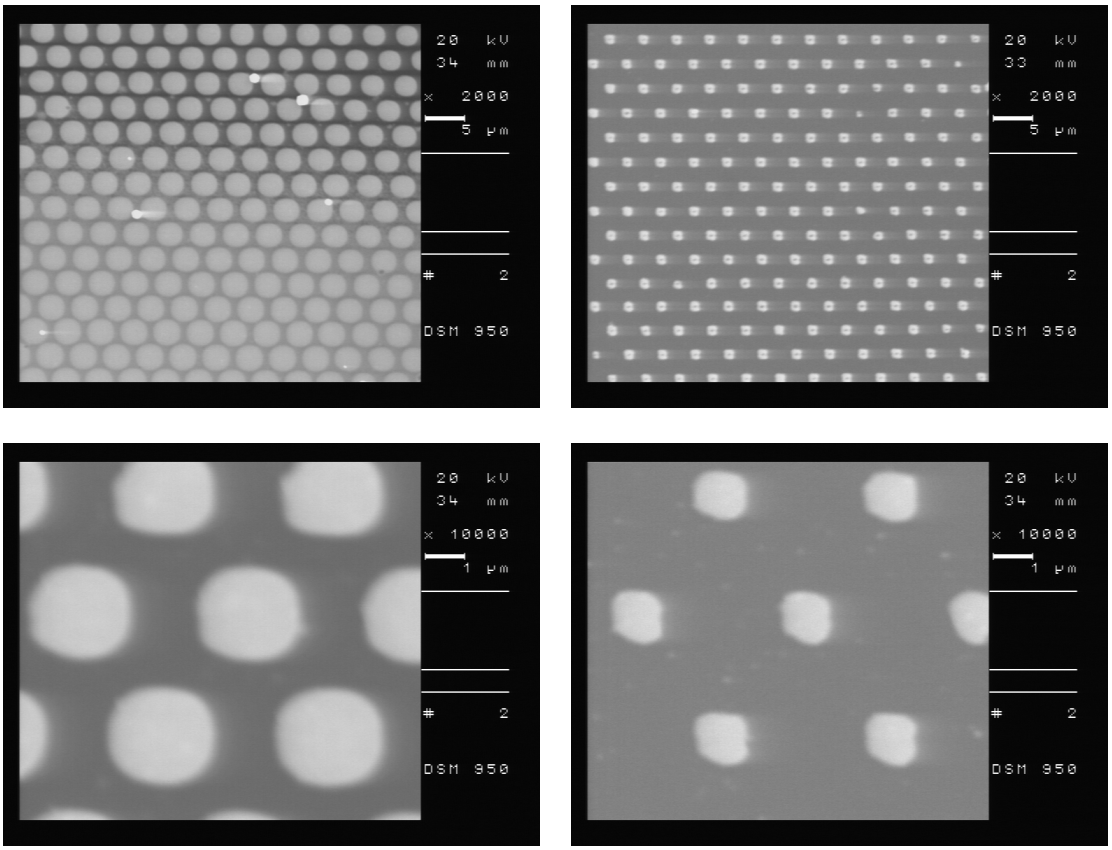

Figure 54. Microcontact printed gold dots on silicon. Wet inking with 0.3sec-stamp. Periodical. variation in the feature size of the print.

In Figure 54, print made with wet inking 0.3sec-stamp, variation in the feature size can clearly be seen. The images are all taken at the central area, but a variation of the size can be clearly seen according to the periodical variation of the pattern.

The results of contact inking experiments with the 0.3sec-stamp are presented in Figure 55. On the left side a pattern at the central area of the print can be seen and on the right a pattern at the edge. As can be seen in Figure 56, the periodical size variation effect is not as visible with contact inking as with wet inking.

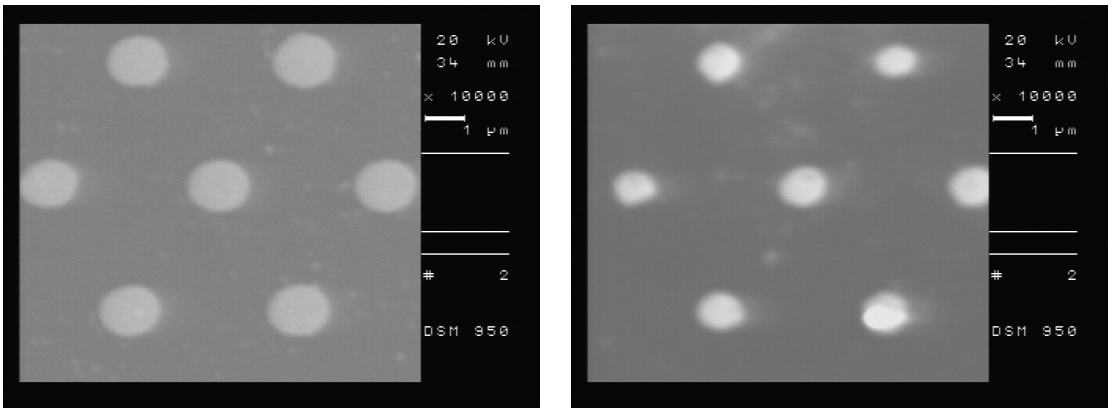

Figure 55. Gold dots on silicon. The printing made with master 0.3sec-stamp, contact inking. The right side figure is at the edge of the stamp where the features are slightly smaller and the left side at the central area.

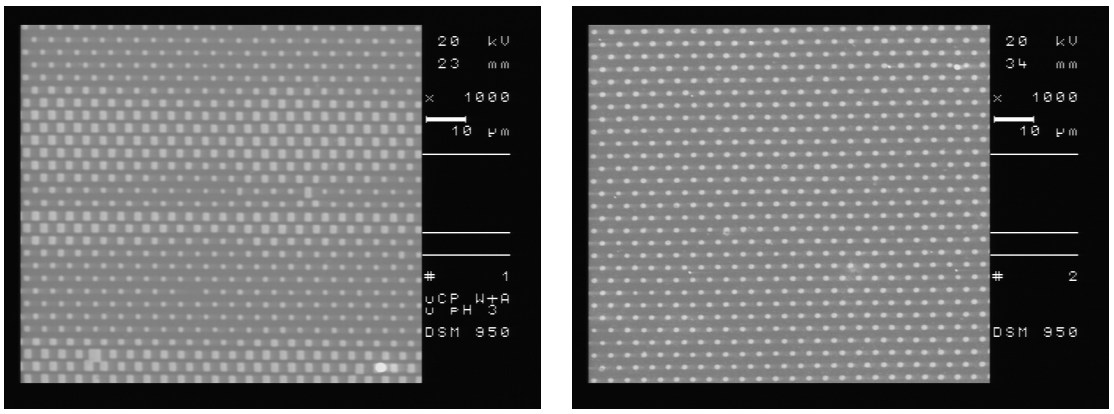

Figure 56. Comparison between wet inking (left) and contact inking (right). Contact inking has better homogeneity in pattern size.

The PDMS 0.3sec-stamp and a contact printed pattern made with this stamp are presented in Figure 57.

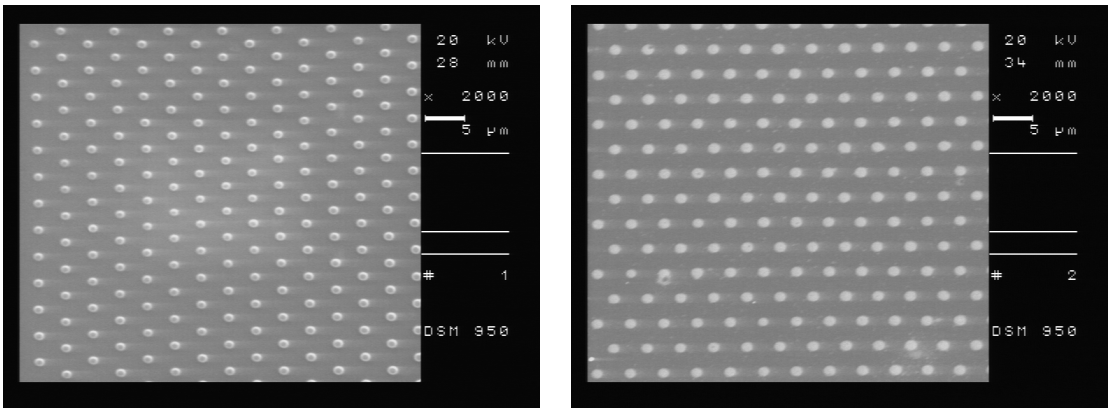

Figure 57. The PDMS 0.3sec-stamp on the left and the printed pattern on the right, contact inking.

The contact inking experiments made with the same stamps as wet inking show that with contact inking the problem with the periodical pattern size variation is less significant than with wet inking. It is however possible that the same periodicity affects also contact inking. These results show, that contact inking produces more regular array of gold dots than wet inking with 0.3sec-stamp.

In conclusion, the 2 µm holes photoresist master design with limiting exposure time in order to create smaller patterns than the original mask pattern is not well suitable for producing homogenous arrays of dots, due to its irregularity in pattern size, especially visible in wet inking. The pattern is not homogenous, but it has a periodical size variation.

5.5.2 Microcontact Printing with Pyramid Stamps

A comparison between wet inking and contact inking with the 10 µm pyramid stamp is presented in Figure 58. Especially in wet inking, the diffusion of the features causes the pattern to be larger than the tip of the pyramid. Using the measurement tool in the scanning electron microscope, the width of a dot is measured to be around 3.5 µm and the tip of the pyramid is measured to be in the range of 500 nm – 1 µm. The contact inking produced a dot size of 1.8 µm.

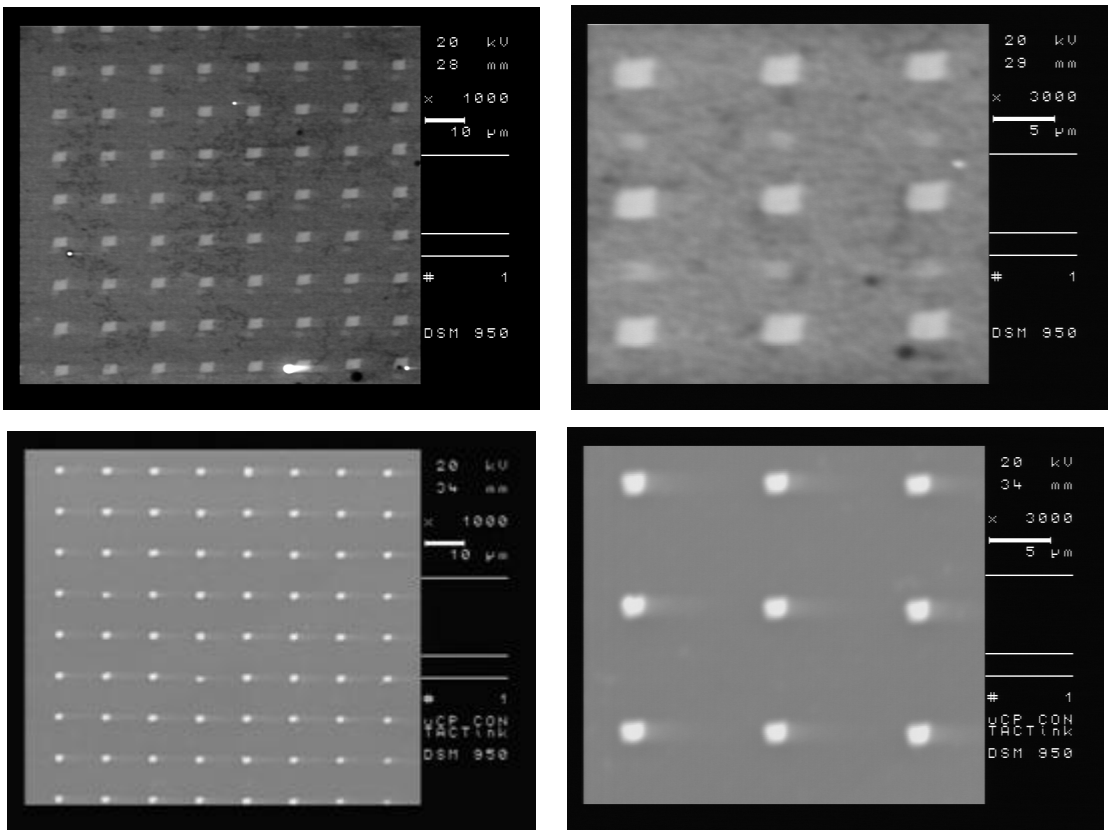

Figure 58. Gold dots on silicon. Print made with the 10 µm pyramid stamp, on the top row: wet inking. The diffusion of the SAMs and thus features can be seen clearly, the size of a gold dot is measured to be around 3.5 µm. On the bottom row: contact inking, the features are smaller with the same magnification as above in wet inking.

The smaller features were printed at the edge of the stamp, as shown in Figure 59. The reason why the smallest gold dots always seemed to appear at the edges of the stamps is yet unclear. The force induced by the weight of the stamp could have been smaller at the edges, causing less contact of the pyramid at the edges. The diffusion would most likely be the same all over the stamp. The etching speed could also have a different rate at different areas of the substrate, or the stirring during etching to cause it to be uneven.

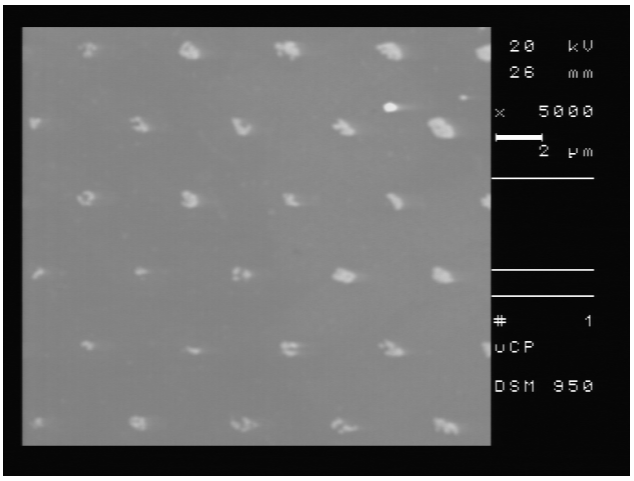

Figure 59. Gold dots on silicon. The smaller patterns at the edges of the stamp area.

5.5.2.1 h-PDMS Composite Bilayer Stamp

The patterns made with a composite stamp are presented in Figure 60.

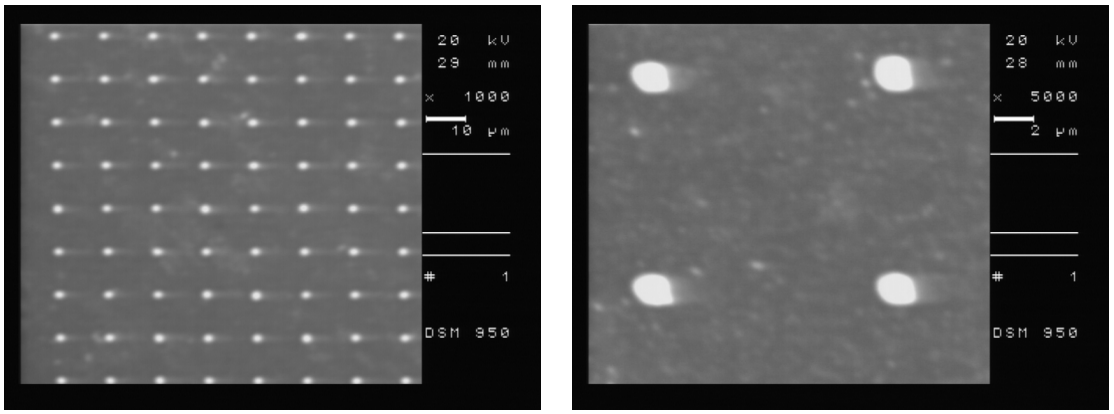

Figure 60. Gold dots on silicon. Print made with h-PDMS pyramid stamp.

The idea of the h-PDMS bilayer composite pyramid stamp was to have a sharper tip so that it could produce smaller features than 184-PDMS stamp, but based on these results, the features are not smaller with the composite stamp when compared with the 184-PDMS stamp. The two printing results, with 184-PDMS and the composite h-PDMS are compared in Figure 61. The size of the dot at the central area is measured to be approximately 1.8 µm, and 1.3 µm at the edge. No notable difference is seen in the images comparing the prints

made with a composite stamp on the right and a regular 184-PDMS stamp. The size of the dot is nevertheless larger than the tip of the pyramid, due to diffusion of the thiols

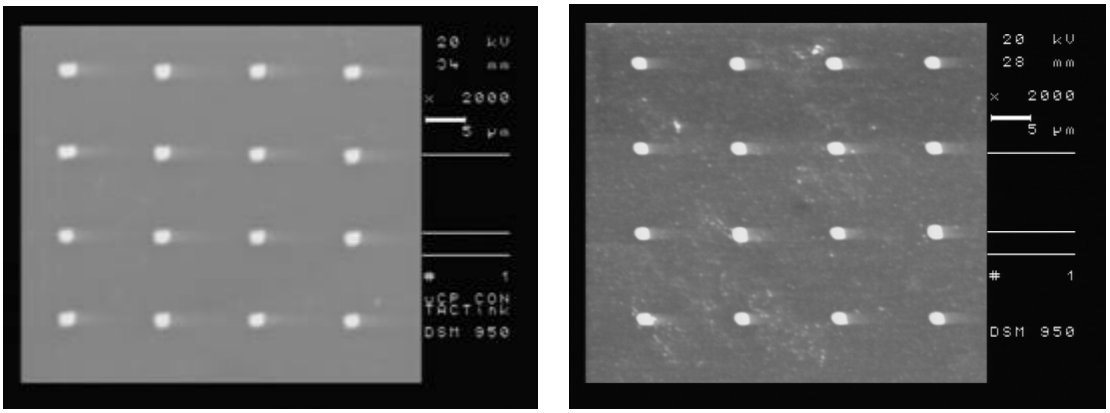

Figure 61. Gold dots on silicon made with the pyramid stamp, contact inking. On the left, 184-PDMS, on the right, h-PDMS composite stamp. Pictures taken at the central area.

5.6 Transfer Printing Results

The stamps chosen for transfer printing experiments were the low aspect ratio stamps. For their nomenclature in this work, refer to Table 9.

5.6.1 Transfer Printing with Low Aspect Ratio Stamps

The 10µm-stamps were used for transfer printing experiments. In Figure 62 it can be seen that the transfer of gold was successful. The gold was transferred from the protruding features of the stamp but remained in the valley areas of the stamp that were not in contact with the substrate. The areas between the squares in the stamp are still gold-coated after printing, as can be seen at the bottom left image in Figure 62. The stamp had approximately a 20 nm layer of gold. When printing, it was very heavily pressed onto the substrate.

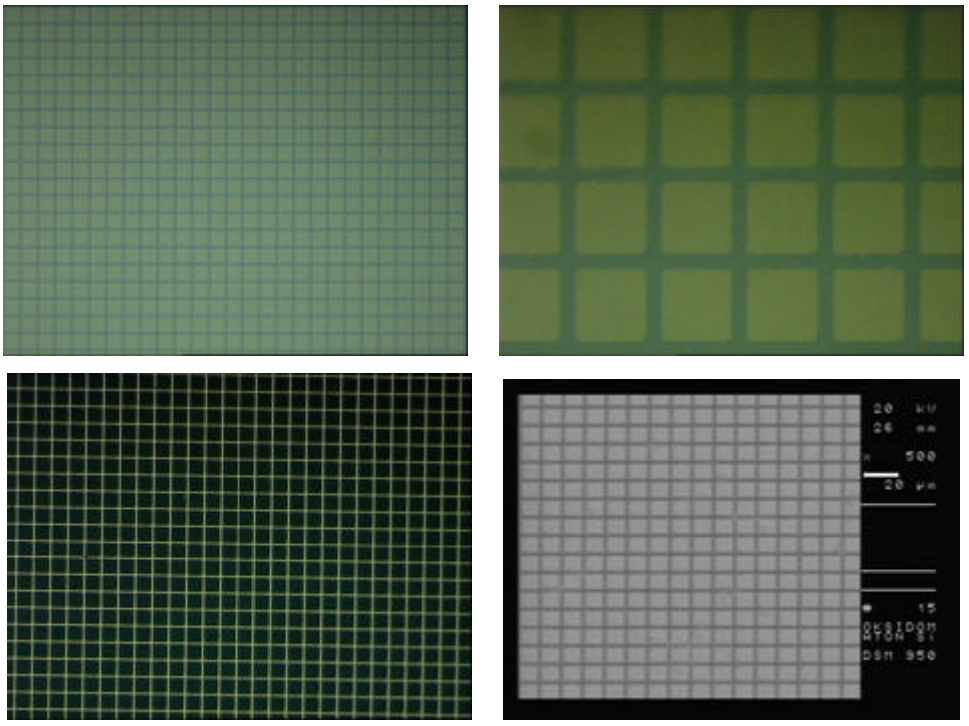

Figure 62. Transfer printing results and the stamp. Top row: transfer printed gold squares created with the 10µm-stamp. Bottom row: the stamp after printing.

The transfer printing results made with the 1.5sec-stamps are presented in Figure 63 and Figure 64.

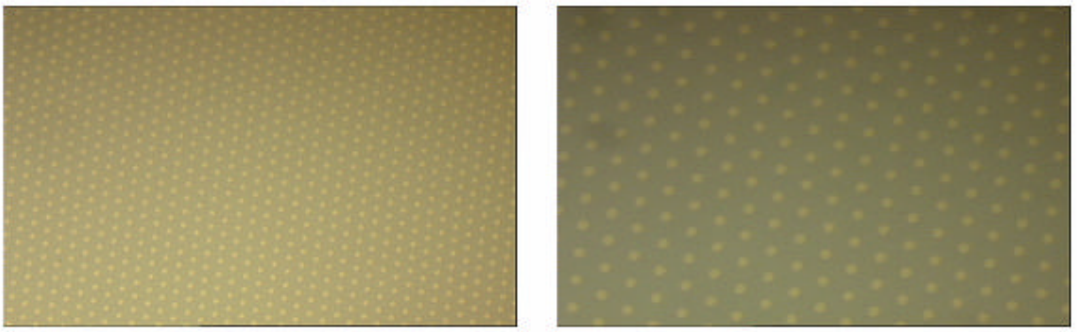

Figure 63. Gold dots on silicon made with transfer printing. 1.5sec-stamp was used for printing.

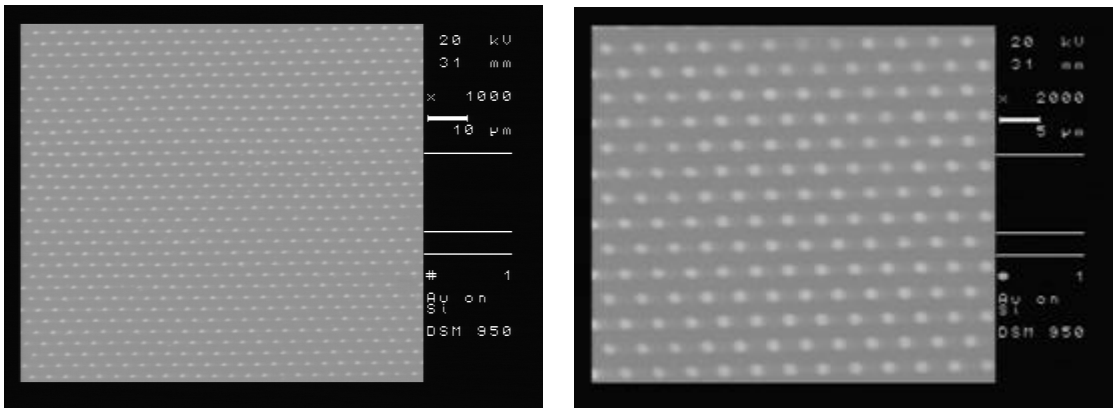

Figure 64. Transfer printing results, gold dots on silicon.

The periodical size variation of the pattern is not visible according to these results. It can be present at some point, however. The pattern looks regular and the edges had the same size of patterns as the central area.

Unlike microcontact printing, force is needed in transfer printing. For the 10µm-stamp with a pitch of 2 µm and the protruding features of 10 µm the force can be used because the valley areas would not touch the substrate. With the 2 µm pillars and 2 µm pitch structures

this can however happen. Too high a force transfers the whole layer of gold, also at the valley areas of the stamp, as shown in Figure 65.

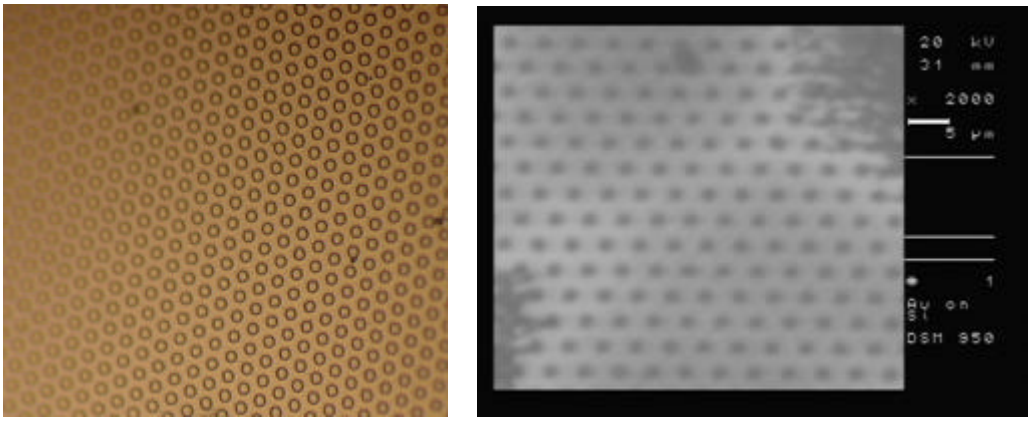

Figure 65. Transfer printing, gold on silicon. When pressed too much, the gold layer also at the valley regions of the stamp comes to contact with the substrate and is transferred.

The transfer printing results with 1sec-stamp and 0.5sec-stamp are presented in Figure 66. According to these images, 0.5sec-stamp produces smaller features than 1sec-stamp.

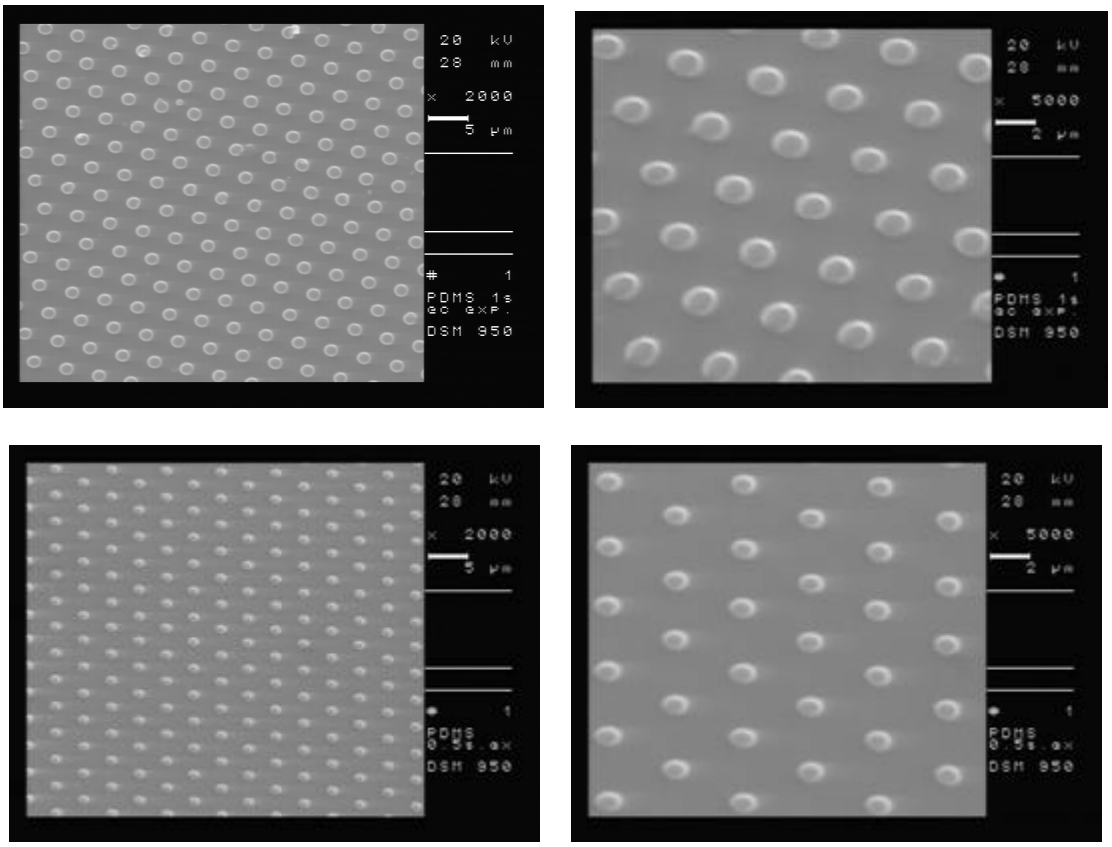

Figure 66. Transfer printed gold dots on silicon. Top row: pattern with 1sec-stamp, bottom row: pattern with 0.5sec-stamp.

In Figure 67 on the left side it can be seen, that the pattern is homogenous and no periodical size variation of the dots is shown, even with the pattern printed with 0.5sec-stamp. On the right side, the size of one transferred gold dot is measured with the SEM measurement tool, to be around 1.2 µm in diameter. This is the smallest size achieved with transfer printing in this work.

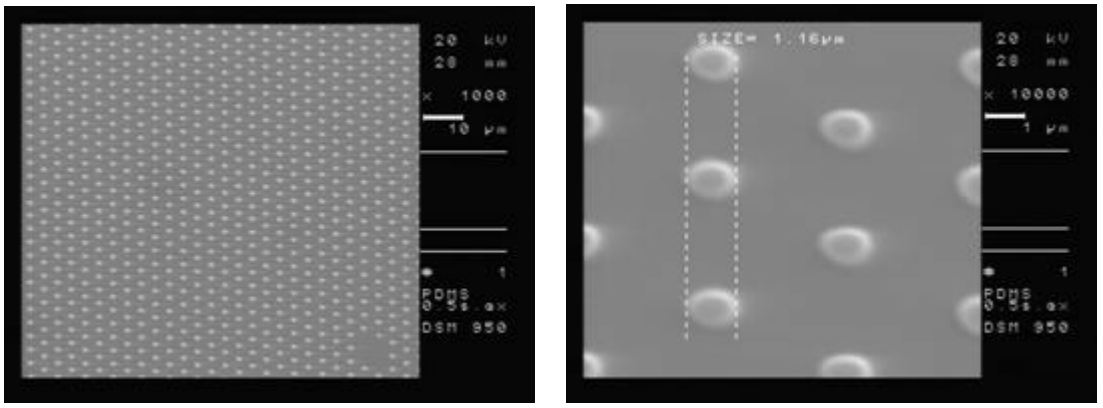

Figure 67. Transfer printing results with a 0.5sec-stamp. The size of a dot is measured to be around 1.2 µm with the measurement tool of SEM.

6 Conclusions and Discussion

In this work the diverse soft lithographic methods were discussed. Different masters were fabricated in order to produce stamps to be used in printing experiments. Microcontact printing and transfer printing experiments were performed in order to produce a regular array of gold dots onto a substrate surface.

Inverted pyramid design, high aspect ratio DRIE design and a low aspect ratio photoresist master design were tested, and elastomeric PDMS stamps fabricated. In the case of a high aspect ratio DRIE master, a release layer was needed in order to enable the removal of the stamp from the master. All of these designs could be used for stamp fabrication.

For microcontact printing experiments, pyramid and low aspect ratio stamps were chosen. The printing experiments were done using both wet and contact inking. The patterns created with the low aspect ratio stamps showed a periodical pattern size variation due to the limitations in the quality of the mask, especially when wet inking was used. Therefore, to create a regular homogenous pattern array, pyramid stamp is better suited.

In microcontact printing, the size of the dots was smaller at the edges of the printed area. This could be due to uneven pressure during printing, or unevenness of the stamp itself; such as distortions in shape of the stamp created during curing or cutting the stamp with a scalpel. To reduce the effect of the edges having smaller features, a more uniform printing pressure should be adjusted, and the evenness of the stamp ensured by better control of its thickness.

Diffusion is a problem with microcontact printing, causing the features to be larger in the print than the features on the stamps. The contact inking method diminishes diffusion, and is thus better suited for patterning small features than wet inking. In order to make the patterns smaller, the diffusion of the thiols should be diminished. This could be done by

further optimising inking and printing times. The etching conditions should also be optimised.

The printing of micrometer scale features outside the clean room is a controversial issue. Therefore some of the samples will be contaminated and thus reducing the quality and yield of the print.

For transfer printing experiments, the low aspect ratio stamp was chosen. The version of transfer printing used in this work differs from the original transfer printing method in the fact that in this work, a self assembled monolayer was not formed onto the substrate surface. The printing was done with a lot of pressure onto the stamp to enable the transfer. The transfer of gold is based on the difference in the adhesion between PDMS-gold and substrate-gold. When the adhesion between substrate and gold is greater than that of the PDMS and gold, the gold layer can be transferred. The printed patterns were overall regular and smooth also at the edges, no periodical size variation was observed, and diffusion is not a problem with transfer printing. Transfer printing is a simpler process than microcontact printing, since etching of the gold is not needed.

For future work in transfer printing, adhesion of the gold layer onto the substrate could be enhanced; an adhesion layer could be tested, such as titanium or chromium on top of the gold that is on the PDMS stamp. This could be tested whether it increases the adhesion of the gold pattern onto the substrate.

In conclusion, microcontact printing and transfer printing both can be used to produce an array of gold dots onto a substrate surface, the dots having a diameter below 2 µm. In microcontact printing, the most regular and homogenous array of the ones tested in this work, is fabricated using pyramid stamps and contact inking. Low aspect ratio stamps are suited for transfer printing.

REFERENCES

1 Y. Xia, J. A. Rogers, K. E. Paul and G. M. Whitesides, "Unconventional methods for fabricating and patterning nanostructures", *Chem. Rev*. **99** (1999) pp.1823-1848

2 S. Franssila: *Introduction to microfabrication*, John Wiley et sons (2004)

3 M. DiVentra, S. Evoy and J. R. Heflin: *Introduction to nanoscale science and technology*, Kluwer Academic Publishers (2004)

4 S. S. Saliterman: *Fundamentals of biomems and medical microdevices*, Wiley Interscience (2006) SPIE press

5 Y. Xia and G. M. Whitesides: "Soft lithography", *Annu. Rev. Mater. Sci.* **28** (1998) pp. 153-184

6 B. D. Gates, Q. Xu, J. C. Love, D. B. Wolfe and G. M. Whitesides, "Unconventional nanofabrication", *Annu. Rev. Mater. Res.* **34** (2004) pp.339-72

7 B. D. Gates, Q. Xu, M. Stewart, D. Ryan, C. G. Willson and G. M. Whitesides: "New approaches to nanofabrication: molding printing and other techniques", *Chem. Rev*. **105**, (2005) pp. 1171-1196

8 Y. Xia and G. M. Whitesides, "Soft lithography", *Angew. Chem. Int. Ed.* **37** (1998) pp. 550-575

9 J. M. K. Ng, I. Gitlin, A. D. Stroock and G. M. Whitesides "Components for integrated poly(dimethylsiloxane) microfluidic systems", *Electrophor.* **23** (2002) pp.3461-3473

10 S.-M. Kim and S. Kang, "Replication qualities and optical properties of UV-moulded microlens arrays", *J. Phys. D: Appl. Phys*. **36** (2003) pp.2451–2456

11 M. Colburn, S. Johnson, M. Stewart, S. Damle, T. Bailey, B. Choi, M. Wedlake, T. Michaelson, S.V. Sreenivasan, J.G. Ekerdt and C.G. Willson. "Step and flash imprint lithography: a new approach to high resolution patterning", *Proc. of SPIE* **3676(I)** (1999): p.379

12 E. Mele, F. Di Benedetto, L. Persano, D. Pisignano and R. Cingolani, "Combined capillary force and step and flash lithography", *Nanotechnology* **16** (2005) pp.391-395

13 S. Y. Chou, P. R. Krauss and P .J. Renstrom: "Imprint of sub-25 nm vias and trenches in polymers", *Appl. Phys. Lett.* **67** (1995) p.3114

14 M. R. Dusseiller, D. Schlaepfer, M. Koch, R. Kroschewski and M. Textor: ”An inverted microcontact printing method on topographically structured polystyrene chips for arrayed micro-3-D culturing of single cells”, *Biomaterials* **26** (2005) pp.5917-5925

15 S. Y. Chou, P. R. Krauss, and P. J. Renstrom, “Nanoimprint lithography”, *J. Vac. Sci. Technol. B* **14** (1996) pp. 4129-4133

16 R. Hull, T. Chraska, Y. Liu and D. Long, “Microcontact printing: new mastering and transfer techniques for high throughput, resolution and depth of focus”, *Mater. Sci. Eng. C* **19** (2002) pp.383–392

17 T. E. Balmer, H. Schmid, R. Stutz, E. Delamarche, B. Michel, N. D. Spencer and H. Wolf: ”Diffusion of alkanethiols in PDMS and its implications on microcontact printing (μCP)”, *Langmuir* **21** (2005) pp.622-632

18 M. Geissler, H. Wolf, R. Stutz, E. Delamarche, U-W. Grummt, B. Michel and A. Bietsch: “Fabrication of metal nanowires using microcontact printing”, *Langmuir* **19** (2003) pp.6301-6311

19 P. C. Hidber, W. Helbig, E. Kim and G. M. Whitesides: ”Microcontact printing of Palladium colloids: micron-scale patterning by electroless deposition of copper”, *Langmuir* **12**(1996) pp.1375-1380

20 B. Michel et al. “Printing meets lithography”, *IBM J. Res. & Dev.* **45**, 5 (2001) pp.697-719

21 S. Jeon, E. Menard, J-U. Park, J. Maria, M. Meitl, J. Zaumseil and J. A. Rogers: ”Three-dimensional nanofabrication with rubber stamps and conformable photomasks”, *Adv. Mater.* **16** (2004) pp.1369-1373

22 W. R. Childs and R .G. Nuzzo: ”Decal transfer microlithography: a new soft-lithographic patterning method”, *J. Am. Chem. Soc.* **124** (2002) 45, pp.13583-13596

23 Y-L. Loo, R. L. Willett, K. W. Baldwin and J. A. Rogers, “Interfacial chemistries for nanoscale transfer printing”, *J. Am. Chem. Soc.* **124** (2002) 26, pp.7654 –7655

24 Y-L. Loo, R. L. Willett, K. W. Baldwin and J. A. Rogers: “Additive, nanoscale patterning of metal films with a stamp and surface chemistry mediated transfer process: applications in plastic electronics”, *Appl. Phys. Lett.* **81** (2002) pp.562-564

25 K. Felmet and Y-L. Loo: “Patterning conductive copper by nanotransfer printing”, *Appl. Phys. Lett.* **85** (2004) pp.3316-3318

26 L.H. Sperling, *Introduction to physical polymer science,* John Wiley et sons (2001)

27 P. C. Powell, *engineering with polymers*, Chapman and Hall Ltd (1983)

28 *Information about high technology silicone materials* Sylgard ® 184 Silicone elastomer base & curing agent, Dow Corning

29 J. C. McDonald and G. M. Whitesides, "Poly(dimethylsiloxane) as a material for fabricating microfluidic devices", *Acc. Chem. Res*. **35** (2002) 7, pp 491-499

30 S. J. Clarson and J. A. Semlyen, *Siloxane polymers*, Prentice hall, Englewood Cliffs, NJ, 1993

31 E. Delamarche, H. Schmid, A. Bietsch, N. B. Larsen, H. Rothuizen, B. Michel and H. Biebuyck, "Transport mechanisms of alkanethiols during microcontact printing of gold", *J. Phys. Chem. B* **102** (1998) pp.3324-3334

32 D. Armani, C. Liu and N. Aluru, "Re-configurable fluid circuits by PDMS elastomer micromachining", *Twelfth IEEE International Conference on Micro Electro Mechanical Systems, 1999, MEMS'99*, pp. 222-227

33 K. M. Choi and J. A. Rogers: "A photocurable poly(dimethylsiloxane) chemistry designed for soft lithographic molding and printing in the nanometer regime", *J. Am. Chem. Soc.* **125** (2003) pp.4060-4061

34 T. Odom, J. C. Love, D. B. Wolfe, K. E. Paul and G. M. Whitesides: "Improved pattern transfer in soft lithography using composite stamps", *Langmuir* **18** (2002) pp.5314-5320

35 H. Schmid and B. Michel:" Siloxane polymers for high-resolution, high-accuracy soft lithography", *Macromol*. **33** (2000) pp.3042- 3049

36 C. Y. Hui, A. Jagota, Y. Y. Lin and E. J. Kramer:" Constraints on microcontact printing imposed by stamp deformation", *Langmuir* **18** (2002) pp.1394-1407

37 Y. Xia, X-M. Zhao and G. M. Whitesides, "Pattern transfer: self-assembled monolayers as ultrathin resists", *Microelectron. Eng.* **32**, (1996) pp. 255-268

38 A. Ulman: "Formation and structure of self-assembled monolayers", *Chem. Rev*. **96**, (1996) pp.1533-1544

39 J. C. Love et al. " Self-assembled monolayers of thiolates on metals as a form of Nanotechnology", *Chem. Rev*. **105**, (2005) 4, pp.1103-1169

40 M. Geissler, H. Wolf, R. Stutz, E. Delamarche, U-W. Grummt, B. Michel and A. Bietsch: "Fabrication of metal nanowires using microcontact printing", *Langmuir* **19** (2003) pp. 6301-6311

41 T. E. Balmer, H. Schmid, R. Stutz, E. Delamarche, B. Michel, N. D. Spencer and H. Wolf: ”Diffusion of alkanethiols in PDMS and its implications on microcontact printing (μCP)”, *Langmuir* **21** (2005) pp. 622-632

42 R. Berger et al “Surface stress in the self-assembly of alkanethiols on gold”, *Science* **276** (1997) pp. 2021 – 2024)

43 Product data sheet of AZ5214E Image reversal photoresist, Clariant GmbH

44 M. Kiuru: ”Experimental studies on diamond-like carbon and novel diamond-like carbon-polymer hybrid coatings”, University of Helsinki, Report series in physics HU-P-D115 (2004)

45 J. E. Mahan*: Physical Vapor Deposition of thin films*, John Wiley et sons, Inc. USA (2000), 312 p

46 L. Libioulle, A. Bietsch, H. Schmid, B Michel and E. Delamarche: ”Contact-inking stamps for microcontact printing of alkanethiols on gold”, *Langmuir* **15** (1999) pp.300-304

Appendix A

Data of the Water Contact Angle Measurement

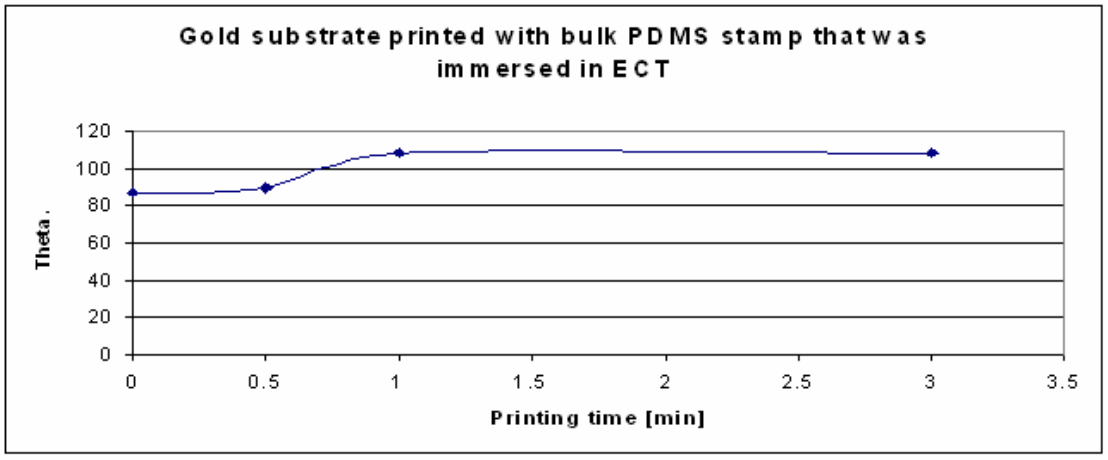

Figure A1. Water contact angle (*theta*) on gold as a function of the immersion time of the gold in 0.2 mM ECT solution.

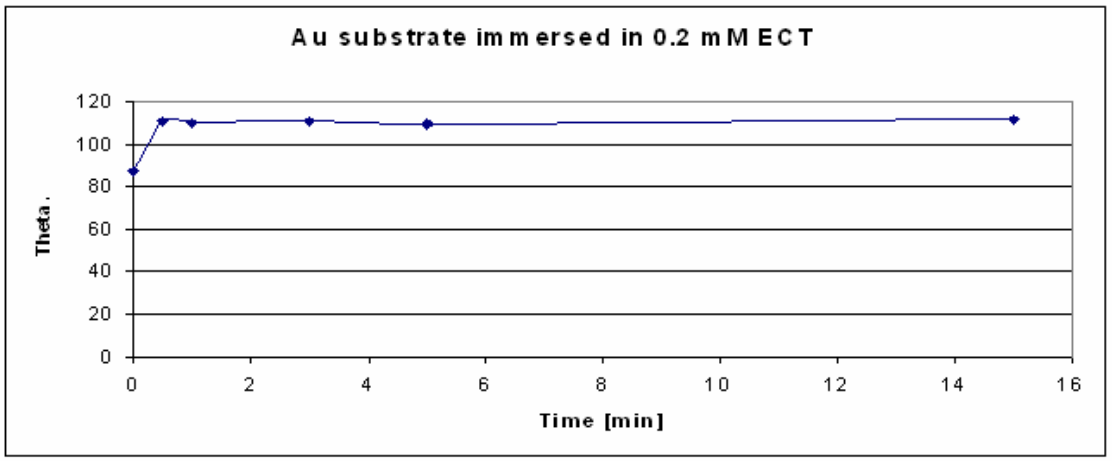

Figure A2. Water contact angle (*theta*) on gold as a function of the printing time with an unpatterned PDMS stamp. The stamp was immersed in 0.2 mM ECT solution.

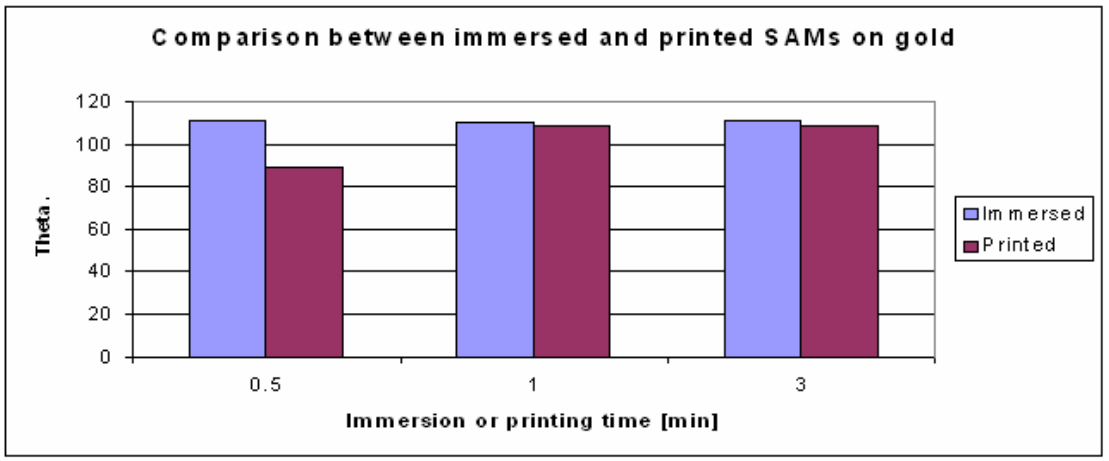

Figure A3. Comparison between the contact angle (*theta*) of SAM on gold formed by immersion of the gold substrate (left pillars) and a SAM for med by printing with an unpatterned stamp (right pillars) .

Source data:

Immersed

time [min]	theta
0	87.486
0.5	110.504
1	110.3033
3	110.635
5	109.3825
15	111.3825

Printed

time [min]	theta
0	87.486
0.5	89.62
1	108.365
3	108.57